Ship Roll Damping Control

Tristan Perez[a,c], Mogens Blanke[b,c]

[a]*School of Engineering, The University of Newcastle, Callaghan NSW 2308, AUSTRALIA.*
[b]*Department of Electrical Engineering, Automation and Control Group, Technical University of Denmark (DTU), DK-2800 Kgs. Lyngby, Denmark.*
[c]*Centre for Ships and Ocean Structures (CeSOS), Norwegian University of Science and Technology (NTNU), Trondheim, NO-7491, NORWAY*

Abstract

The technical feasibility of roll motion control devices has been amply demonstrated for over 100 years. Performance, however, can still fall short of expectations because of difficulties associated with control system designs, which have proven to be far from trivial due to fundamental performance limitations and large variations of the spectral characteristics of wave-induced roll motion. This tutorial paper presents an account of the development of various ship roll motion control systems together with the challenges associated with their design. It discusses the assessment of performance and the applicability of different mathematical models, and it surveys the control methods that have been implemented and validated with full scale experiments. The paper also presents an outlook on what are believed to be potential areas of research within this topic.

Keywords: Ship Motion Control, Ship Roll Stabilisation, Ship Roll Damping.

1. Introduction

Roll motion can affect the performance of seagoing surface vessels by limiting the effectiveness of the crew, damaging cargo, and limiting the operation of on-board equipment. From William Froude's observations on roll motion, which lead to the proposal of bilge keels in the late 1800s, to the present, various devices have been proposed and used to reduce ship roll motion. Most of these stabilisation devices rely on feedback control systems whose designs have proven to be far from trivial and subject to fundamental performance limitations and trade-offs combined large variations of the spectral characteristics of wave-induced roll motion.

The technical feasibility of roll motion control devices has been amply demonstrated for over 100 years. After the last addition of rudder roll damping systems in the 1970s, most of the work shifted to developments in control system design rather than to the development of new stabilisation concepts. Recently, however, there has been a surge in revitalising roll gyrostabilisers and a proposal for zero-speed fin stabilisers. These developments have been pushed by the luxury yacht industry. In addition, there are currently several navies pursuing again the use of rudder-roll damping systems.

This tutorial paper presents an account of the development of various ship roll motion control systems together with the challenges associated with their design. It discusses the assessment of performance, the applicability of different models, and the control methods that have been

applied in the past. It also presents an outlook on what are believed to be potential areas of research within this topic.

2. Ship Dynamics and Roll Motion

The dynamics of marine vessels can be described using the following general model structure (Fossen, 1994):

$$\dot{\boldsymbol{\eta}} = \mathbf{J}(\boldsymbol{\eta})\,\boldsymbol{\nu}, \tag{1}$$

$$\mathbf{M}_{RB}\,\dot{\boldsymbol{\nu}} + \mathbf{C}_{RB}(\boldsymbol{\nu})\boldsymbol{\nu} = \boldsymbol{\tau}_h + \boldsymbol{\tau}_c + \boldsymbol{\tau}_d, \tag{2}$$

where the vector variables $\boldsymbol{\eta}$ and $\boldsymbol{\nu}$ represent the generalised displacement and body-fixed velocities, and $\boldsymbol{\tau}_h$, $\boldsymbol{\tau}_c$, and $\boldsymbol{\tau}_d$ represent the hydrodynamic, control and disturbance forces respectively. To describe the vessel motion, a reference frame $\{b\}$ is considered fixed to the vessel at the point o_b, and a local geographical frame $\{n\}$ is considered fixed to the mean water level at the location o_n. These reference frames are illustrated in Figure 1. The generalised position and velocity vectors are given by

$$\boldsymbol{\eta} = [n, e, d, \phi, \theta, \psi], \tag{3}$$

$$\boldsymbol{\nu} = [u, v, w, p, q, r]^T. \tag{4}$$

The components of $\boldsymbol{\eta}$ are the north, east and down positions of o_b with respect to $\{n\}$ and the Euler angles ϕ (roll), θ (pitch), and ψ (yaw), which take $\{n\}$ into the orientation of $\{b\}$. The components of $\boldsymbol{\nu}$ are the linear velocities expressed in the body-fixed frame, namely, u-surge, v-sway, and w-heave. The components of angular velocity vector expressed in the body-fixed frame are the p (roll rate), q (pitch rate), and r (yaw rate). The generalised force vectors in the body-fixed frame are given by

$$\boldsymbol{\tau}_i = [X_i, Y_i, Z_i, K_i, M_i, N_i]^T, \tag{5}$$

where X_i is the surge force, Y_i is the sway force, Z_i is the heave force, K_i is the roll moment, M_i is the pitch moment, and N_i is the yaw moment. All the moments are taken about o_b.

The kinematic transformation $\mathbf{J}(\boldsymbol{\eta})$ relates the body-fixed velocities to the time derivative in $\{n\}$ of the generalised positions, which gives the vessel trajectory. The matrix $\mathbf{M}_{RB}$ in (2) is the rigid-body mass matrix, and $\mathbf{C}_{RB}(\boldsymbol{\nu})$ is the Coriolis-centripetal matrix. The term $\mathbf{C}_{RB}(\boldsymbol{\nu})\boldsymbol{\nu}$ in Eq. 2 appears as a consequence of expressing the velocity vector ion a rotating (non-inertial) frame. For further details about general models of marine vessels see Fossen (1994), Fossen (2002), Fossen (2011) or Perez (2005).

The study of roll motion dynamics for control system design is normally done in terms of either one or four degrees of freedom (DOF) models. The choice between models of different complexity depends on the type of motion control system considered and the conditions under which the design is to be performed. There may be cases where a full six degree of freedom model is required.

2.1. One degree of freedom Model

For a one-degree-of-freedom (1DOF) model in roll, the model (1)-(2) can be reduced to the following form

$$\dot{\phi} = p, \tag{6}$$

$$I_{xx}\,\dot{p} = K_h + K_c + K_d, \tag{7}$$

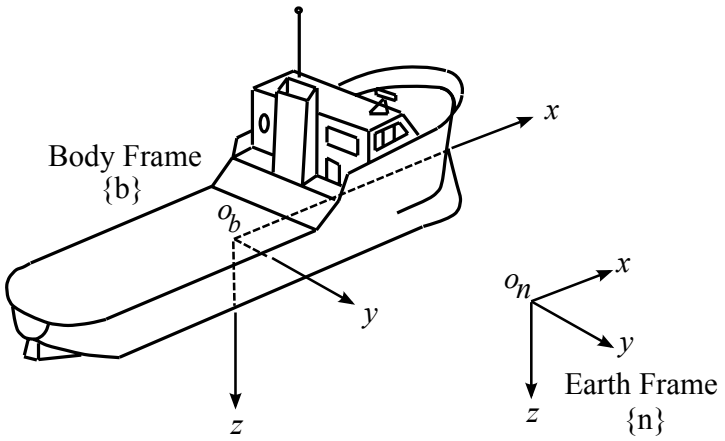

Figure 1: Reference frames used for ship motion description.

where I_{xx} is the rigid-body moment of inertia about the x-axis of $\{b\}$. This model assumes that the formulation is about the centre of roll. The hydrodynamic forces can be approximated by the following parametric model:

$$K_h \approx K_{\dot{p}}\,\dot{p} + K_p p + K_{p|p|}\,p|p| + K(\phi). \tag{8}$$

The first term on the right-hand side of (8) represents a hydrodynamic moment in roll due to pressure change that is proportional to the roll accelerations, and the coefficient $K_{\dot{p}}$ is called roll added mass. The second term is a damping term, which captures forces due to wave making and linear skin friction, and the coefficient K_p is called a linear damping coefficient. The third term is a nonlinear damping term, which captures forces due to viscous effects, like nonlinear skin friction and eddy making due to flow separation. The last term is a restoring term due to gravity and buoyancy, which for some vessels a linear approximation often suffice:

$$K(\phi) \approx K_\phi\,\phi, \qquad K_\phi = \rho\, g\, \nabla\, GMt, \tag{9}$$

where ρ is the water density, g is the acceleration of gravity, ∇ is the vessel displaced volume, and GMt is the transverse metacentric height (Lewis, 1988a,b).

The coefficients in the hydrodynamic model (8) change with the forward speed of the vessel U. This can be represented in the model by adding terms; for example

$$K_h \approx K_{h0} + K_{hU}, \tag{10}$$

where

$$K_{h0} = K_{\dot{p}}\,\dot{p} + K_p p + K_{p|p|}\,p|p| + K(\phi), \tag{11}$$

$$K_{hU} = K_{Up}\,Up + K_{\phi UU}\,\phi U^2, \tag{12}$$

$$\tag{13}$$

As the forward speed changes, so does the trim of the vessel, which can be related to the steady state pitch angle. The trim affects not only the damping but also the restoring term (9). Some vessels have trim tabs—see Figure 2—which are used to correct the trim at different cruise speeds so as to reduce the hydrodynamic resistance and thus fuel consumption. The use of trim tabs modify the restoring coefficient (9).

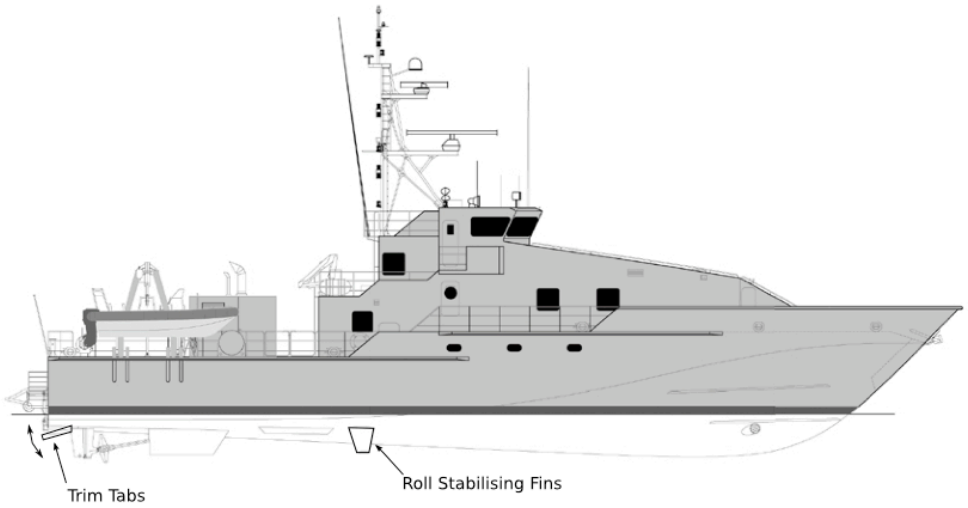

Figure 2: Roll stabilising fins and trim-tabs. Picture courtesy of Austal, Australia.

2.2. *Four degree of freedom Model*

For a 4DOF model (surge, sway, roll, and yaw), motion variables considered are

$$\boldsymbol{\eta} = [\phi\ \psi]^T, \tag{14}$$

$$\boldsymbol{\nu} = [u\ v\ p\ r]^T, \tag{15}$$

$$\boldsymbol{\tau}_i = [X_i\ Y_i\ K_i\ N_i]^T, \tag{16}$$

The kinematic model (1) reduces to

$$\dot{\phi} = p, \qquad \dot{\psi} = r\cos\phi \approx r. \tag{17}$$

The rigid-body mass and Coriolis-centripetal matrices are given by

$$\mathbf{M}_{RB} = \begin{bmatrix} m & 0 & 0 & -my_g \\ 0 & m & -mz_g & mx_g \\ 0 & -mz_g & I^b_{xx} & -I^b_{xz} \\ -my_g & mx_g & -I^b_{zx} & I^b_{zz} \end{bmatrix}, \tag{18}$$

and

$$\mathbf{C}_{RB}(\nu) = \begin{bmatrix} 0 & 0 & mz_g r & -m\left(x_g r + v\right) \\ 0 & 0 & -my_g p & -m\left(y_g r - u\right) \\ -mz_g r & my_g p & 0 & I^b_{yz} r + I^b_{xy} p \\ m\left(x_g r + v\right) & m\left(y_g r - u\right) & -I^b_{yz} r - I^b_{xy} p & 0 \end{bmatrix}, \tag{19}$$

where m is the mass of the vessel, $[x_g, y_g, z_g]^T$ gives position the centre of gravity relative to o_b, and I^b_{ik} are the moments and products of inertia about o_b.

The hydrodynamic forces can be expressed as

$$\boldsymbol{\tau}_h \approx -\mathbf{M}_A\,\dot{\boldsymbol{\nu}} - \mathbf{C}_A(\boldsymbol{\nu})\boldsymbol{\nu} - \mathbf{D}(\boldsymbol{\nu})\boldsymbol{\nu} - \mathbf{K}(\phi). \tag{20}$$

The first two terms on the right-hand side of (20) can be explained by considering the motion of the vessel in an irrotational flow and for ideal fluid (no viscosity). As the vessel moves, it changes momentum of the fluid. By considering the kinetic energy of the fluid as $T = 1/2\,\boldsymbol{\nu}^T \mathbf{M}_A \boldsymbol{\nu}$, the first two terms in (8) follow from Kirchhoff's equations—see Lamb (1932) and Fossen (1994). The third term in (20) corresponds to damping forces due to potential (wave making), skin friction, vortex shedding, and circulation (lift and drag). The hydrodynamic effects involved are often too complex to model with lumped parametric models. Hence, different approaches based on superposition of either odd-term Taylor expansions or square modulus ($x|x|$) series expansions are usually used as proposed by Abkowitz (1964) and Fedyaevsky and Sobolev (1964) respectively. The last term in (20) represents the restoring forces in roll due to buoyancy and gravity, which for the degrees of freedom being considered, it reduces to (9).

The added mass matrix and the Coriolis-centripetal matrix due to added mass are given by

$$\mathbf{M}_A = \mathbf{M}_A^T = -\begin{bmatrix} X_{\dot{u}} & 0 & 0 & 0 \\ 0 & Y_{\dot{v}} & Y_{\dot{p}} & Y_{\dot{r}} \\ 0 & K_{\dot{v}} & K_{\dot{p}} & K_{\dot{r}} \\ 0 & N_{\dot{v}} & N_{\dot{p}} & N_{\dot{r}} \end{bmatrix}, \tag{21}$$

$$\mathbf{C}_A(\boldsymbol{\nu}) = -\mathbf{C}_A(\boldsymbol{\nu})^T = \begin{bmatrix} 0 & 0 & 0 & Y_{\dot{v}} v + Y_{\dot{p}} p + Y_{\dot{r}} r \\ 0 & 0 & 0 & -X_{\dot{u}} u \\ 0 & 0 & 0 & 0 \\ -Y_{\dot{v}} v - Y_{\dot{p}} p - Y_{\dot{r}} r & X_{\dot{u}} u & 0 & 0 \end{bmatrix}. \tag{22}$$

The adopted damping terms take into account lift, drag, and viscous effects.

$$\mathbf{D}(\boldsymbol{\nu}) = \mathbf{D}_{LD}(\boldsymbol{\nu}) + \mathbf{D}_V(\boldsymbol{\nu}),$$

where

$$\mathbf{D}_{LD}(\boldsymbol{\nu}) = \begin{bmatrix} 0 & 0 & 0 & X_{rv}\, v \\ 0 & Y_{uv}\, u & 0 & Y_{ur}\, u \\ 0 & K_{uv}\, u & 0 & K_{ur}\, u \\ 0 & N_{uv}\, u & 0 & N_{ur}\, u \end{bmatrix}. \tag{23}$$

$$\mathbf{D}_V(\boldsymbol{\nu}) = \begin{bmatrix} X_{u|u|} & 0 & 0 & 0 \\ 0 & Y_{|v|v}\,|v| + Y_{|r|v}\,|v| & 0 & Y_{|v|r}\,|v| + Y_{|r|r}\,|r| \\ 0 & 0 & K_{p|p|} + K_p & 0 \\ 0 & N_{|v|v}\,|v| + N_{|r|v}\,|v| & 0 & N_{|v|r}\,|v| + N_{|r|r}\,|r| \end{bmatrix}. \tag{24}$$

The lift-drag representation (23) is consistent with taking only the 1st order terms derived by Ross (2008), whereas the viscous damping representation (24) follows from Blanke (1981), which is a simplification of the model proposed by Norrbin (1970). Some other models appearing in the literature can have additional terms. In the above damping model we have included all the terms with physical meaning. When these models are derived from data of captive scale-model tests, the coefficients are obtained from regression analysis, and further terms may be incorporated to best fit the experimental data (Blanke and Knudsen, 2006; Perez and Revestido-Herrero, 2010).

2.3. Higher-order Dynamics Due to Radiated Waves

The 4DOF model described in the previous section is called a *manoeuvring model*, since it can be used to describe vessel manoeuvring characteristics. The hydrodynamic forces are modelled on the assumption that there is no waves. The motion in waves is usually studied under the assumption that the vessel is not manoeuvring and thus the waves induce a perturbation motion about a steady state sailing condition given by a constant speed and heading. This leads to a so-called *seakeeping model*, which captures wave excitation forces and also the effects of radiated waves as a consequence of the motion of the vessel. The latter effects are captured in the equations of motion as high-order dynamics related to the *radiation forces* which can be approximated using a linear time-invariant model (Perez and Fossen, 2008b,a, 2007). The problem of manoeuvring in waves is still the subject of ongoing research since it is difficult to approach with simplified theories. For control design, it is common to consider a combination of manoeuvring models from control forces to motion, and to use seakeeping models to generate output disturbances related to wave-induced motion. The output disturbance model is obtained by taking realisation of the wave-induced roll motion spectrum. This is discussed in the next sections.

2.4. Ocean Waves

Ocean waves are random in time and space. The underlying stochastic model assumes that the observed sea surface elevation $\zeta(t)$ relative to the mean level at a certain location is a realisation of a stationary and zero mean Gaussian stochastic process (Ochi, 1998). Under the stationary and Gaussian assumptions, the sea surface elevation is completely characterised by its Power Spectral Density (PSD) $\Phi_{\zeta\zeta}(\omega)$, commonly referred to as the *wave spectrum*. This contains all the information regarding the sea state since the mean of wave elevation is zero, and the variance is given by area under the spectrum over the range of frequencies $(0, \infty)$. The wave spectrum is often narrow banded, and uni-modal. However, there could be cases of multi-modal spectra when there are wind-waves (high frequency) and swell (low frequency) present. Figure 3 shows an example of an idealised unimodal wave spectrum normally used for ship motion evaluation. For further details see Ochi (1998).

When a marine craft is at rest, the frequency at which the waves excite the craft coincides with the wave frequency observed from an earth-fixed reference frame. When the craft moves with a constant forward speed U, however, the frequency observed from the craft differs from the wave frequency. The frequency experienced by the craft is called the *encounter frequency*. The encounter frequency depends not only on speed of the craft, but also on angle of waves' approach:

$$\omega_e = \omega - \frac{\omega^2 U}{g}\cos(\chi). \tag{25}$$

where, the encounter angle χ defines the sailing condition, namely, Following seas (χ= 0deg), Quartering seas ($0 < \chi < 90$ deg), Beam seas ($\chi = 90$ deg), Bow seas ($90 < \chi < 180$ deg), and Head seas ($\chi = 180$ deg). The encounter frequency captures a Doppler effect, and this is important since the ship motion response due to wave excitation depends on the frequency. As shown by Price and Bishop (1974), the wave spectrum observed from the sea is

$$\Phi_{\zeta\zeta}(\omega_e) = \frac{\Phi_{\zeta\zeta}(\omega)}{\left|\frac{d\omega}{d\omega_e}\right|} = \frac{\Phi_{\zeta\zeta}(\omega)}{\left|1 - \frac{2\omega U}{g}\cos(\chi)\right|},$$

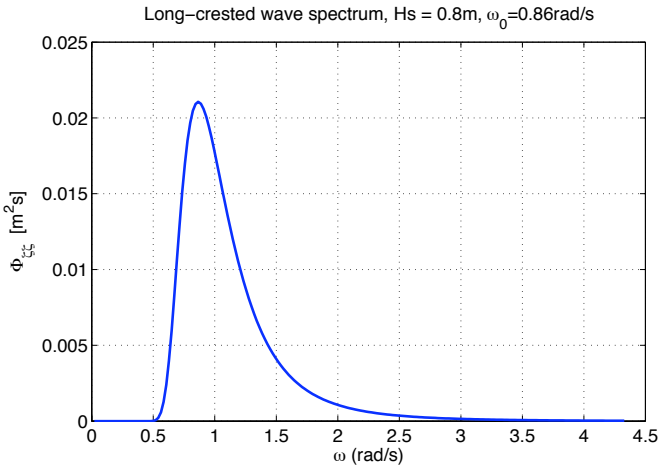

Figure 3: Example of idealised wave spectrum (ITTC) for significant wave height H_s =0.8m (average of 1/3 of the highest waves) and modal period ω_0 = 0.86rad/s.

which follows from the fact the energy of wave elevation is invariant with respect to frame of reference in which the waves are observed.

2.5. Wave-induced Forces and Motion—Output-disturbance Models

The motion of a marine craft in waves is the result of changes in the pressure on the hull. The wave excitation forces, as well as the vessel response, will depend not only on the characteristics of the waves—amplitude and frequency—but also on the *sailing conditions*: encounter angle and speed. Based on linear potential theory, hydrodynamic software is nowadays readily available for the computation of the following frequency response functions:

- $\mathbf{F}(j\omega, \chi, U)$ - Wave elevation to excitation force.
- $\mathbf{G}(j\omega, U)$ - Wave excitation to motion.

These frequency responses, known in marine literature as *Response Amplitude Operators* (RAOS) are computed based on linearisation at an equilibrium condition defined by a constant forward speed U and encounter angle χ. Because the motion is in 6DOF,

$$\mathbf{F}(j\omega,\chi) = \begin{bmatrix} F_1(j\omega,\chi,U) & \cdots & F_6(j\omega,\chi,U) \end{bmatrix}^T, \tag{26}$$

$$\mathbf{G}(j\omega,U) = \begin{bmatrix} G_{11}(j\omega,U) & \cdots & G_{16}(j\omega) \\ \vdots & & \vdots \\ G_{61}(j\omega,U) & \cdots & G_{66}(j\omega,U) \end{bmatrix}, \tag{27}$$

where the degrees of freedom are identified as 1-surge, 2-sway, 3-heave, 4-roll, 5-pitch, and 6-yaw.

From the above frequency response functions, one can obtain the wave to motion response:

$$\mathbf{H}(j\omega,\chi,U) = \mathbf{G}(j\omega,U)\,\mathbf{F}(j\omega,\chi,U). \tag{28}$$

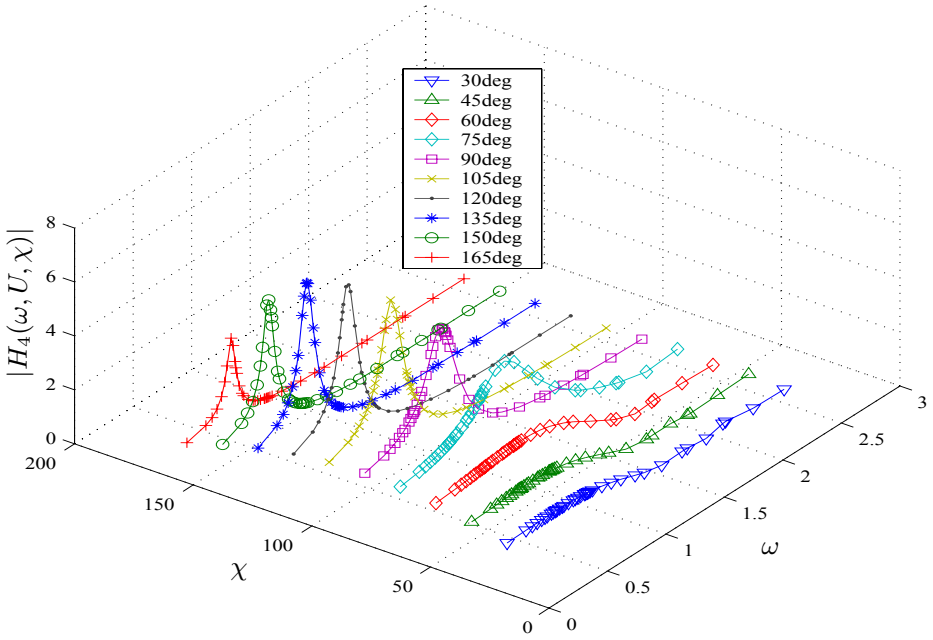

Figure 4: Roll RAOs of a navy vessel at 15kts for different encounter angles (Perez, 2005).

such that

$$\delta\boldsymbol{\eta}(j\omega) = \mathbf{H}(j\omega, \chi, U)\zeta(j\omega),$$

where the notation $\delta\boldsymbol{\eta}(j\omega)$ indicates that these are perturbations from the equilibrium state. The response for the degree of freedom i is given by

$$H_i(j\omega, \chi, U) = \sum_{k=1}^{6} G_{ik}(j\omega, U)F_k(j\omega, \chi, U). \tag{29}$$

Figure 4 shows the roll response of a naval vessel for different encounter angels (Perez, 2005). As apparent from this figure, changes in wave encounter angle can have a significant impact on ship roll motion. This often poses a problem for roll motion control design since the wave-induced forces and motion are likely to change over a wide range of frequencies depending on sea state and sailing conditions (Blanke et al., 2000a).

Having the frequency responses (26)-(27), one can combine them with the wave spectrum to obtain the spectrum of the wave-induced motion:

$$\Phi_{\eta\eta,i}(j\omega_e) = |H_i(j\omega_e, \chi, U)|^2 \Phi_{\zeta\zeta}(j\omega_e). \tag{30}$$

This spectrum can used to simulate time series of wave-induced motion. Since the wave elevation is Gaussian and considered stationary, and the force response being considered is linear, then the response is also Gaussian and stationary. One approach to generate realisations from the spectrum consists of making a spectral factorisation of (30) and approximate the realisations as

filtered white noise. This approach is commonly used in stochastic control theory. An approach commonly used in naval architecture is to use a multi-sine signal. For example for any component of η_i, we can generate realisations via

$$\eta_i(t) = \sum_{n=1}^{N} \bar{\eta}_n \cos(\omega_{e,n} t + \varepsilon_n), \tag{31}$$

with N being sufficiently large, where $\bar{\eta}_n$ are constants, and the phases ε_n are independent identically distributed random variables with uniform distribution in $[0,\ 2\pi]$. This choice of random phases ensures that $\eta_i(t)$ is a Gaussian process, and for each realisation of the phases, we obtain a realisation of the process (St Denis and Pierson, 1953). The amplitudes are determined from $\bar{\eta}_n = \sqrt{2\Phi_{\eta\eta,i}(\omega^*)\Delta\omega}$, where ω^* is chosen randomly within the interval $[\omega_n - \frac{\Delta\omega}{2}, \omega_n + \frac{\Delta\omega}{2}]$. For further details about wave induced forces and motion for control see Perez (2005).

3. Roll Motion and Ship Performance

Roll affects ship performance in terms of preventing the operation of on-board equipment, human performance, and in some case it affects the efficiency of the propulsion system. Transverse accelerations due to roll induce interruptions in the tasks performed by the crew. This increases the amount of time required to complete the missions, and in some cases may even prevent the crew from performing tasks at all. This can render navy ships inoperable (Monk, 1988). Vertical accelerations induced by roll at locations away from the ship's centre line can contribute to the development of seasickness in the crew and passengers, which affects performance by reducing comfort. Roll accelerations may produce cargo damage, for example on soft loads such as fruit. Large roll angles limit the capability to handle equipment on board. This is important for naval vessels performing weapon operations, launching or recovering systems, landing airborne systems, and sonar operation.

Within the naval environment, several performance indices and associated criteria are used to quantify ship performance relative to the missions it performs. Among the different performance indices,the following are affected by roll motion (NATO, 2000):

- maximum roll angle, roll angle dependent propeller emergence,
- vertical acceleration, acceleration dependent lateral force estimator,
- motion sickness incidence and motion induced interruptions.

The main point is that the performance of a roll motion control system must be judged not only in terms of roll angle reduction, but also roll accelerations.

4. A Historical Account on Roll Damping Devices

The undesirable effects of roll motion became noticeable in the mid-19th century when significant changes were introduced to the design and development of ships. Sails were replaced by steam engines, and for warships, the arrangement was changed from broadside batteries to turrets (Goodrich, 1969). The combination of these changes, in particular the dropping of sails, led to modifications of the transverse stability with the consequence of large roll motion. The increase in roll motion and its effect of ship and human performance lead to several different devices that

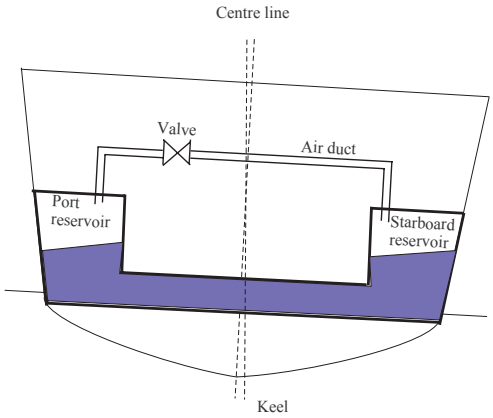

Figure 5: U-tank.

aim at reducing and controlling roll motion. The devices most commonly used today are water tanks, gyrostabilisers, fins, and rudder.

In 1878, a committee in England presented a study on damaged stability for the *HMS Inflexible*, in which they concluded that the free flow of the water within the damaged compartments contributed to an increase of roll righting power. This happened only if the number of partially flooded compartments was low and the level of water appropriate (Chalmers, 1931; Goodrich, 1969). As a result of these experiments, the *HMS Inflexible* was permanently fitted with water chambers in 1880 (Watt, 1883, 1885). This, together with the work of Froude, was probably the earliest attempt of using passive anti-rolling tanks. This work was followed by the development of the U-tank made by Frahm (1911). This U-tank was found to be more effective than the free-surface tank previously used by Froude and Watt. As shown in Figure 5, a U-tank consists of two reservoirs located one on the starboard side and the other on the port side. These reservoirs are connected via a duct that allows the flow from one reservoir to the other. This type of anti-roll tank is still very much in use to date. The tanks are dimensioned so that the tank's natural frequency matches the vessel roll natural frequency. This can only be achieved at a single frequency. Therefore, performance degradation occurs if the motion of the vessel departs from the natural frequency. This can be circumvented by active control. Work on active anti-roll tanks started in the 1930s. For example, Minorsky (1935) used a pump to alter the natural flow in the tanks in 1934. The velocity of the fluid was varied according to the roll acceleration. During the 1960s and 1970s there was significant research activity to better understand the performance of these stabilisers, see for example, Vasta et al. (1961); Goodrich (1969) and references therein. More complete passages on the history and the development of anti-roll tanks, which also includes contemporary references, can be found in Chalmers (1931); Vasta et al. (1961); Goodrich (1969); Gawad et al. (2001). In particular, the work of Vasta et al. (1961), summarises the early development of stabilisers within the US Navy, which did not take place until the 1930s. This reports the use of tanks in different vessels, and provides a mathematical model of a U-tank based on the developments made at Stanford University in the early 1950s. To date, the control is performed by controlling the air pressure on the upper side of the reservoirs via a valve.

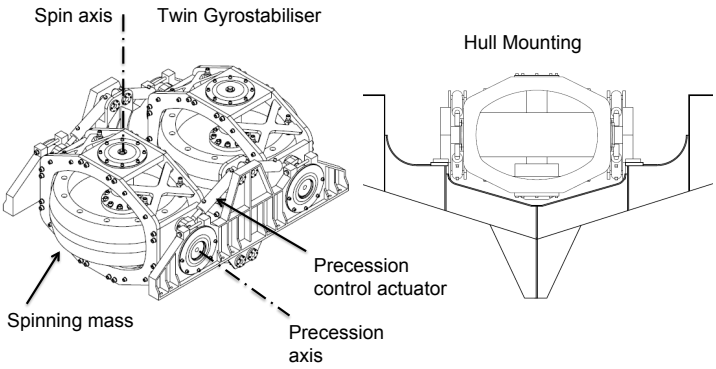

Figure 6: Example of twin-wheel gyrostabiliser.

The use of gyroscopic forces was then proposed as a method to eliminate roll rather than reducing it. A gyrostabiliser consists of one or more dedicated spinning wheels whose gyroscopic effects are used to counteract roll excitation forces. An example of such device is depicted in Figure 6. Schlick (1904) was the first to propose use of the gyroscopic effects of large rotating wheels as a roll control device. In 1907, this system was installed on the ex-German torpedo-boat destroyer *See-Bar*. The Schlick gyroscope presented some problems in adjusting its performance according to the magnitude and frequency of the waves, and although it worked well for the vessel used by Schlick, it did not perform as expected in other vessels—see Chalmers (1931) for details. The American company Sperry then developed a system that addressed the problem of the Schlick gyroscope by using an electrical motor commanded by switches and a small gyroservo to control the precession of the main gyroscope. In this, the velocity of precession was proportional to the roll rate of the vessel. Although the performance of these system was remarkable, up to 95% roll reduction, their high cost, the increase in weight and large stress produced on the hull masked their benefits and prevented further developments. In recent years, there has been a increase the development of gyrostabilisers driven by the yacht industry and the need to stabilise roll motion at anchor (Perez and Steinmann, 2009).

Fin stabilisers consist of a pair of controlled hydrofoils mounted on the side of the hull, which are commanded by a control system to produce a roll moment that counteracts the wave induced moment—see Figure 2. The first proposal for fin stabilisers was made by S. Motora of the Mitsubishi Nagasaki Shipyard in Japan, in 1923 (Chalmers, 1931). The use of active-fin stabilisers increased after World War II. This was a consequence of the combined work of the Denny and the Brown Brothers companies in England, but the idea of using fin stabilisers was developed before the war. To date fin stabilisers are also used at zero forward speed–flapping fins.

The idea of using the rudder as a stabilisation device emerged from observations of ship roll behaviour under autopilot operation. Taggart (1970) reported an unusual combination of circumstances occurring on the *American Resolute* (container ship) during a winter Atlantic crossing in 1967, which resulted in excessive ship rolling when automatic steering was used. From data observed during that trip and a model constructed from data of a summer crossing in 1968, it was concluded that the high roll motion observed, even in the absence of significant seaway, was the consequence of high yaw frequencies, which made the autopilot produce rudder activity close

to the roll natural frequency of the ship. It was then suggested that the autopilot control system should be modified to avoid these effects; however, the fact that rudder motion could produce large roll could be used as anti-rolling device. Motivated by the observations, van Gunsteren performed full-scale trials using the rudder as a stabiliser in 1972 aboard the motor yacht *M.S. Peggy* in Ijsselmeer (inner waters of The Netherlands). This work was reported by van Gunsteren (1974). Independently from the above work, Cowley and Lambert (1972) presented a study of rudder roll stabilisation using analog computer simulations and model testing of a container ship in 1972. Subsequent sea trials following this work were reported in Cowley (1974); Cowley and Lambert (1975), the latter with encouraging results. This work, obtained on commercial ships, motivated the exploration of rudder stabilisers in the naval environment in the United Kingdom. Carley (1975) and Lloyd (1975a) reported their studies, in which they analysed not only the benefits but also the complications associated with the control of rudder stabilisers. This work seems to have been the first rigorous attempt to analyse performance limitations of rudder stabilisers. Although the idea of using the rudder as a roll stabilising mechanism ignited in the early 1970s, the performance obtained was, in general, poor. This was mainly because of the simple control strategies attempted, due to the limitations imposed by the analog computers. It was only in the 1980s that more advanced control algorithms, and digital computers made more successful experimental results possible: Baitis reported roll angle reductions of 50% in 1980—see Baitis (1980). After this, most of the successful implementations were reported towards the end of the 1980s and beginning of the 1990s—see for example the work of van der Klught, van der Klught (1987), Källström (1981), Källström et al. (1988), Blanke et al. (1989) and van Amerongen et al. (1990). These developments were mostly within the naval environment.

The above is a brief review on the main developments of stabilisation concepts adapted from Perez (2005). Sellars and Martin (1992) provides a comparison between different devices in terms of performance and cost.

5. Motion Control and Performance Limitations

Active control of roll motion by means of force actuators can usually be addressed within a linear framework, from the control loop depicted in Figure 7. The output sensitivity transfer function is,

$$S(s) \triangleq \frac{\phi_{cl}(s)}{\phi_{ol}(s)}, \tag{32}$$

where $\phi_{cl}(s)$ and $\phi_{ol}(s)$ are the Laplace transforms of the closed- and open-loop roll angles respectively. Note that the same sensitivity transfer function holds for the roll accelerations. In terms of power spectral densities, the following relationship holds,

$$\Phi_{\phi_{cl}\phi_{cl}} = |S(j\omega)|^2 \, \Phi_{\phi_{ol}\phi_{ol}}. \tag{33}$$

Based on (33), the control objective is the reduction of the sensitivity within the range of frequencies where the roll motion occurs.

When the single-input-single output system of Figure 7 is stable and strictly proper, the Bode's integral constraint, due to the feedback structure, establishes that,

$$\int_0^\infty \log |S(j\omega)| \, d\omega = 0. \tag{34}$$

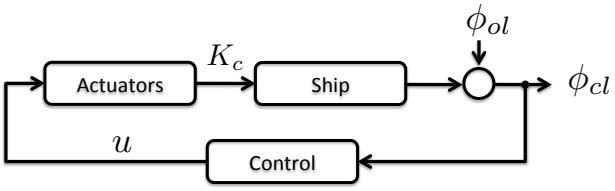

Figure 7: Schematic of a SISO roll control loop with open-loop wave-induced roll motion as output disturbance

This constraint indicates that a reduction of the magnitude of the sensitivity below 1 at some frequencies must result in an increase at other frequencies. By defining the roll reduction as

$$RR(\omega) = 1 - |S(j\omega)| = \frac{|\phi_{ol}(j\omega)| - |\phi_{cl}(j\omega)|}{|\phi_{ol}(j\omega)|}, \tag{35}$$

the integral constraint becomes

$$\int_0^\infty \log(1 - RR(\omega))\, d\omega = 0. \tag{36}$$

Furthermore, the open- and closed-loop responses from wave-induced moment to roll angle are,

$$G_{ol}(s) = \frac{\phi_{ol}(s)}{\tau_w(s)}, \tag{37}$$

$$G_{cl}(s) = \frac{\phi_{cl}(s)}{\tau_w(s)}. \tag{38}$$

Using these functions the roll reduction is,

$$RR(\omega) = \left(1 - \frac{|G_{cl}(j\omega)|}{|G_{ol}(j\omega)|}\right). \tag{39}$$

We note that $G_{ol}(s)$ depends only on the vessel characteristics, i.e., hydrodynamic aspects and mass distribution. Hence, the integral constraint (36) imposes restrictions on one's freedom to shape the function $G_{cl}(s)$ to attenuate the motion due to the wave induced forces in different frequency ranges. These results have important consequences on the design of a control system. Since the frequency of the waves seen from the vessel change significantly with the sea state, the speed of the vessel, and the heading with respect to the wave propagation direction. The changing characteristics on open-loop roll motion in conjunction with the integral constraint (34) make the control design challenging since roll amplification may occur if the control design in not done properly.

For some roll motion control problems, like rudder roll damping, the system presents non-minimum phase dynamics. This effect is related to the location of the force actuator and the coupling between different degrees of freedom—roll, sway and yaw. In these cases, there is an integral constraint similar to (34) but the sensitivity reduction-amplification trade off is concentrated to frequency regions in the neighbourhood of the real right half plane (RHP) zero (non-minimum phase zero) located at $s = q$:

$$\int_{-\infty}^{\infty} \log|S(j\omega)|\, W(q,\omega)\, d\omega = 0, \tag{40}$$

where

$$W(q,\omega) = \frac{q}{q^2+\omega^2}. \tag{41}$$

The formal prerequisite here is again that the open-loop transfer function of plant and controller has relative degree strictly larger than one and that the open loop system has no poles in the right half plane. Both criteria are met for the rudder to roll transfer function of a vessel with positive metacentric height. The weighting function $W(q,\omega)$ is referred to as the Poisson Kernel, and the above integral is known as the Poisson integral constraint for stable single-single-output feedback systems (Serón et al., 1997).

From the constraints (34) and (40), one can obtain bounds on the maximum of the sensitivity that can be expected outside the attenuation range $\Omega_a = [\omega_{min}, \omega_{max}]$. That is if the control requirement is

$$|S(j\omega)| \leq \alpha, \quad \text{for } \omega \in \Omega_a, \tag{42}$$

then,

$$1 \leq \|S(j\omega)\|_\infty \leq \gamma(q, \Omega_a, \alpha), \ \text{ for } \omega \notin \Omega_a. \tag{43}$$

For the problem of rudder roll damping these bounds were first investigated by Hearns and Blanke (1998a)—see also Perez (2005).

It should be noted that non-minimum phase dynamics also occurs with fin stabilisers, when the stabilisers are located aft of the centre of gravity. With the fins at this location, they behave like a rudder and introduce non-minumum phase dynamics and significant heading interference at low wave encounter frequencies. These aspects of fin location were discussed by Lloyd (1989).

The above discussion listed general design constraints that apply to roll motion control systems in terms of the dynamics of the vessel and actuator. In addition to these constraints, one needs also to account for limitations due to actuator capacity. The topic of fundamental limitations is further discussed in the following sections.

6. Control Design using Fin Stabilisers for Roll Damping

Provided that the fin location is such that there is no non-minimum phase dynamics, the control design for fin stabilisers can be performed based on a single degree freedom model,

$$\dot{\phi} = p, \tag{44}$$

$$[I_{xx} + K_{\dot{p}}]\,\dot{p} + K_p\, p + K_{|p|p}\,|p|p + K_\phi\,\phi = K_w + K_f, \tag{45}$$

where K_w is wave induced roll moment and K_f is the roll moment induced by the fins.

The lift and drag forces of the hydrofoils are concentrated at the centre of pressure (CP) and can be modelled as

$$\begin{aligned} L &= \frac{1}{2}\rho V_f^2 A_f \bar{C}_L \alpha_e \\ D &= \frac{1}{2}\rho V_f^2 A_f \left(C_{D0} + \frac{(\bar{C}_L \alpha_e)^2}{0.9\pi a} \right), \end{aligned} \tag{46}$$

where V_f is the flow velocity upstream from the foil, A_f is the area of the foil, α_e is the effective angle of attack in radians, and a is the effective aspect ratio. In (46), we have used the linear approximation for the lift coefficient:

$$\bar{C}_L = \left.\frac{\partial C_L}{\partial \alpha_e}\right|_{\alpha_e=0},$$

which is valid for $\alpha_e < \alpha_{stall}$. Once the stall angle of the hydrofoils is reached, the flow separates and the lift reduces.

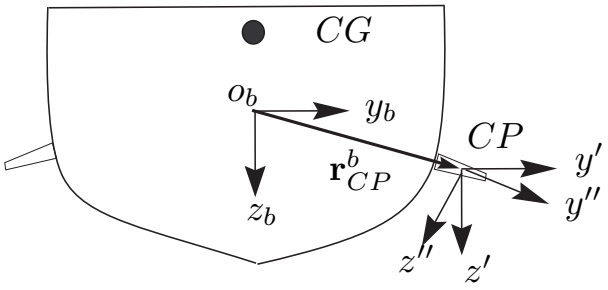

Figure 8: Reference frames used to compute fin forces.

The lift force is perpendicular to the direction of the relative flow, whereas the drag force is aligned with the relative flow. The computation of the roll moment due to these forces requires taking into account the complete motion of the vessel and fin rotation. This is a complex problem. To calculate the forces, we consider the reference frames depicted in Figure 8, and we assume that the location of the centre of pressure of the fin in body-fixed coordinates is given by the vector $\mathbf{r}^b_{CP} = [x^b_{CP}, y^b_{CP}, z^b_{CP}]^T$.

If we neglect the influence of pitch and heave motion, then the relative flow in frame x'', y'', z'' is

$$\mathbf{v}_f = [-U, 0, -r_f\, p]^T, \quad r_f = \sqrt{(y^b_{CP})^2 + (z^b_{CP})^2}, \tag{47}$$

where U is the forward speed of the vessel (assumed constant), and we are assuming the vessel centre of roll is at the origin of the body-fixed frame. The angle of the flow relative to x'', y'', z'' is defined as

$$\alpha_f = \arctan \frac{r_f p}{U} \approx \frac{r_f p}{U}, \tag{48}$$

and the effective angle of attack is given by

$$\alpha_e = -\alpha_f - \alpha, \tag{49}$$

where α is the mechanical angle of the fin, defined positive defined using the right-hand-screw rule along the y'' axis: a positive angle means leading edge up: trailing edge down.

The lift and drag forces in x'', y'', z'' are

$$\mathbf{F}_{LD} = [D, 0, L]^T, \tag{50}$$

and the roll moment can then be expresses as

$$X_f = [1, 0, 0]\, \mathbf{S}(\mathbf{r}^b_{CP})\, \mathbf{R}_{x,\gamma}\, \mathbf{F}_{LD}, \tag{51}$$

where $\mathbf{R}_{x,\gamma}$ is the rotation matrix that takes the b-frame into the orientation of x'', y'', z'' (which we assume that the tilt angle is γ about the x-axis), and $\mathbf{S}(\mathbf{r}^b_{CP})$ is the skew-symmetric matrix

associated with the vector $\mathbf{r}^b_{CP}$. After, calculations, and further approximating $\|\mathbf{v}_f\| \approx U$, we obtain that

$$X_f \approx U^2 K_\alpha \, \alpha_e, \tag{52}$$

where

$$K_\alpha = \frac{1}{2}\rho A_f (y^b_{CP} \cos\gamma - z^b_{CP} \sin\gamma). \tag{53}$$

From the above, the model finally is,

$$\dot{\phi} = p, \tag{54}$$

$$[I_x + K_{\dot{p}}]\, \dot{p} + (K_p + 2\, r_f K_\alpha U)\, p + K_{|p|p}\, |p| p + K_\phi \phi = K_w - 2U^2 K_\alpha \alpha. \tag{55}$$

As seen from the model (55), the presence of the fins increase the bare damping of the hull, and the damping as well as the effectiveness of the fins are affected by the forward speed.

From the point of view of control design, the main issues are the parametric uncertainty in (55) and the integral constraints (34), which applies if only roll angle feedback is used. The integral constraint can lead to roll amplification due to changes in the spectrum of the wave-induced roll moment with sea state and sailing conditions. Fin machinery is normally designed so the rate of the fin motion is fast enough so there are no issues of actuator rate saturation. The fins can be used to correct heeling angles (steady state roll). This is achieved by integral action in the controller—which requires anti wind-up implementation to avoid performance degradation due actuator saturation in magnitude.

Classical PID and $\mathcal{H}_\infty$ types of controllers usually perform well for fin stabiliser control (Hickey et al., 1995, 1997, 1999; Hickey, 1999; Katebi et al., 2000), and most of the early literature on fin stabilisation focused strongly on the hydrodynamic aspects of the fins, fin size and location rather than control design (Allan, 1945; Conolly, 1969; Lloyd, 1975b; Dallinga, 1993).

Crossland (2003) performed a study of performance for a particular naval vessel mission and compared two tuning methods for PID controller (classical and optimal) and an $\mathcal{H}_\infty$ control design. The classical design follows the procedure of Lloyd (1989), which provides maximum roll reduction at the vessel natural frequency. The design has the following specifications in terms of the output sensitivity transfer function at specific frequencies:

- Low-frequency upper bound: $|S(\omega_l)| \leq 2$ dB
- Resonance: $|S(\omega_r)| \leq -16$ dB
- High-frequency upper bound: $|S(\omega_h)| \leq 6$ dB
- Phase margin $\geq$ 45deg

The optimal PID tuning followed the procedure of Katebi et al. (2000), which optimised the value of the control gains subject to the above constraints. The $\mathcal{H}_\infty$ optimal control followed the procedure of Sharif et al. (1996), which uses frequency-dependent weights for the output sensitivity, complementary sensitivity, and control sensitivity. The latter takes into account that the actuators have a limited bandwidth. Interestingly, the study reported by Crossland (2003) showed very little different in the performance of these three controllers. It could be argued that this is attributed to the fundamental limitations associated with integrals of the sensitivities of the control design, which hold for any stable strictly proper loop system.

The study of hydrodynamic aspects of fin stabilisers have continued to attract research attention until recent years due to tendency of fins to develop dynamic stall conditions in moderate to

severe sea states (Gaillarde, 2002). This latter work has motivated the control strategy proposed in Perez and Goodwin (2008), which considers a constraint on the effective angle of attach to prevent dynamic stall.

Although the traditional approach for the design of fin stabiliser control consists of using the decoupled roll motion equations, the cross-coupling between roll, sway and yaw often reduces the performance of the fins, and therefore if the system as a whole is to operate optimally, and integrated control for rudder and fin should be considered. Furthermore, if the fins are located aft, the a non-minimum phase dynamics can appear in the response due to coupling with yaw, which can complicate the controller design and compromise the performance at low encounter frequencies. Non-minimum phase dynamics in fin-roll response and the design trade-offs due to integral constrain (40) were mentioned by Lloyd (1989), and discussed by Perez (2005) and Perez and Goodwin (2008). Full-scale experiments have been reported by Sharif et al. (1996) and a study for a naval vessel which shows the benefits of the integrated approach can be found in Crossland (2003).

7. Control Design using Rudder(s) for Roll Damping

As mentioned in Section 4, using the rudder for simultaneous steering and roll damping has been investigated for several decades. Early results demonstrated the importance of available rudder rate to achieve desired roll damping. Implementation on a number of vessels in different countries showed limitations to achievable roll reduction. A full understanding of the limits due to dynamics of the problem was not available until results on achievable performance for systems appeared Freudenberg and Looze (1985) and further elaborated and extended in Freudenberg and Looze (1988) and Serón et al. (1997).

The linearised transfer function from rudder angle to roll angle obtained from the 4DOF model specified in Section 2.2 is

$$G_{\phi\delta}(s) = \frac{c_{\phi\delta}(1 + s\tau_{z1})(1 - \frac{s}{q})}{(1 + s\tau_{p1})(1 + s\tau_{p2})(\frac{s^2}{\omega_p^2} + 2\zeta_p \frac{s}{\omega_p} + 1)} \tag{56}$$

If the output disturbance d_ϕ (wave-induced roll motion) is to be attenuated, *i.e.* $\log|S(j\omega)| < 0$ (or equivalently $|S(j\omega)| < 1$) in a range of frequencies $\omega \in \Omega$, then there must be amplification of disturbances at frequencies outside Ω, *i.e.* for $\omega \notin \Omega$, $\log|S(j\omega)| > 0$ (or $|S(j\omega)| > 1$). Furthermore, due to the weighting factor in the integral (40), this balance of area has to be achieved over a limited band of frequencies, which depend on the position of the RHP zero q.

Suppose that the feedback loop is to be designed to achieve

$$|S(j\omega)| \leq \alpha_1 < 1\,, \qquad \forall\omega \in \Omega_1 = [\omega_1, \omega_2]. \tag{57}$$

Define,

$$\Theta_\sigma(\omega_1, \omega_2) \triangleq \int_{\omega_1}^{\omega_2} \frac{q}{q^2 + \omega^2}\, d\omega = \arctan\frac{\omega_2}{q} - \arctan\frac{\omega_1}{q}. \tag{58}$$

Dividing the range of integration in (40), and using the inequality (57) and also the fact that $|S(j\omega)| \leq \|S(j\omega)\|_\infty$ for all ω, we obtain that

$$\ln\alpha_1\ \Theta_\sigma(\omega_1, \omega_2) + \log\|S(j\omega)\|_\infty\,[\pi - \Theta_\sigma(\omega_1, \omega_2)] \geq 0. \tag{59}$$

By exponentiating both sides of (59), it follows that

$$\|S(j\omega)\|_\infty \geq \left(\frac{1}{\alpha_1}\right)^{\frac{\Theta_\sigma(\omega_1,\omega_2)}{\pi-\Theta_\sigma(\omega_1,\omega_2)}}. \tag{60}$$

Thus, the right-hand side of (60) is a lower bound on the sensitivity peak that will be expected outside the range $[\omega_1, \omega_2]$. It is immediate from (60) that the lower bound on the sensitivity peak is strictly greater than one: this follows from the fact that $\alpha_1 < 1$ and $\Theta_q(\omega_1, \omega_2) < \pi$. Furthermore, the more the sensitivity is pushed down, i.e., the lower is α_1, and the bigger is the interval $[\omega_1, \omega_2]$, then the bigger $\|S(j\omega)\|_\infty$ will be at frequencies outside that interval.

The above description of the disturbance attenuation problem has been formulated from a deterministic point of view. The use of frequency response is particularly attractive to consider sinusoidal disturbances. Indeed, if the frequency of the disturbance is not known exactly, then the reduction of the sensitivity should be considered over a range of frequencies where the disturbance is likely to be. The price to pay for doing this is an increase of sensitivity outside the range of reduction, and the risk of disturbance amplification if the disturbance is indeed outside the reduction range.

7.1. Limits of achievable performance

With a fixed controller for rudder roll damping, there is the risk that for some sailing conditions and sea states, the disturbances have significant energy in the frequency ranges where roll is amplified. This is more likely to happen in quartering sailing conditions for which low encounter frequencies result. This would mean having a disturbance with significant energy at frequencies below ω_1 in Eq. 57. This limitation was recognised since the first attempts to use rudder as a roll damping device were made—see Carley (1975); Lloyd (1975a) but the stringent mathematical background was not disclosed until much later, when the analysis of performance limitations due to the RHP zero was approached using the Poisson integral formula was first discussed by Hearns and Blanke (1998a).

In order to study limitations, Perez (2005) took a state-feedback approach, and formulated the control problem as a limiting optimal control problem, in which the following cost was minimised

$$J = \mathrm{E}[\lambda\phi^2 + (1-\lambda)(\psi - \psi_d)^2], \tag{61}$$

where $\mathrm{E}[\cdot]$ is the expectation operator, and $\lambda \in [0, 1]$ represents the desired of reducing roll over yaw deviations. When $\lambda = 1$, it was established that

$$\mathrm{E}[\phi^2] \geq 2\, q\, \Phi_{\phi_{ol}\phi_{ol}}(q), \tag{62}$$

Expression (62) shows that the closer the RHP zero, q, is to the imaginary axis, the better are the chances for a rudder stabiliser to perform well. A RHP zero close to the imaginary axis will produce a large initial inverse response to a rudder step command. The fact that a large initial inverse response to a step in the rudder command is an indication of the potential for good performance of a rudder stabiliser has been discussed by Roberts (1993). Therefore, the location of the RHP zero with respect to the imaginary axis gives a *definite* and *quantitative* interpretation for the statement constantly appearing in the literature which says that for a rudder stabiliser to perform well there must be a frequency separation between the roll and yaw responses due to the rudder action. Indeed, if the zero is close to the imaginary axis, this means that there will

be a timelag in the development of the hydrodynamic moment acting on the hull that opposes that produced by the rudder. For a given ship, the location of the RHP zero is determined by its hydrodynamic characteristics related to hull shape, rudder location, and mass distribution. The relation between hydrodynamic parameters was derived from PMM data for a container vessel by Hearns and Blanke (1998b).

Equation (62) also shows another important aspect: a RHP zero close to the imaginary axis does not *per se* guarantee good performance; there must also be a frequency separation between the RHP zero and the bulk of power of the wave-induced roll motion in order to achieve good performance. This answers the question as to why RRD systems can have significantly different performance under different sailing conditions, with poor performance being particularly noticeable at low-encounter frequencies.

The bound on the right-hand side of (62) is very conservative because there is no penalty in the control energy used. One of the main issues with rudder roll damping control is the limitation imposed by the attainable rate by the rudder actuator. This produced a saturation that can severely degrade the performance of the control system due to a lag. van Amerongen et al. (1990) proposed the use an automatic gain control (AGC) to limit the rudder command. This idea was borrowed from radio receivers

$$\alpha_{acg} = \frac{\dot{\alpha}_{max}}{\max[\dot{\alpha}_{max}, |\dot{\alpha}_c|, y(t-\Delta)]}\,\alpha_c,$$

where α_c is the output of the controller, and α_{agc} is the attenuated command send to the actuators.

Since the limitations due to the actuator can dominate the performance in some sailing conditions, Perez et al. (2003) developed a bound imposing a constraint on the variance of the rudder angle, such that the maxima of rudder angle exceed a certain threshold value with low probability. For example, Figure 9 shows the achievable performance for the case of a naval vessel in beam seas. The bottom plot shows an approximation of the open-loop roll angle spectrum, and the top plot shows the curves of roll reduction and yaw due to the action of the RRD controller for the case of constrained and unconstrained rudder forces. This plot was obtained by varying the parameter λ in (61). It is interesting to notice that in this example the limitations are mostly dominated by capacity of the rudder to produce roll moment. For the case where the open loop roll spectrum shifts to lower frequencies, the difference between constrained and un-constrained performance becomes smaller, since the the limitations are dominated by the non-minimum phase dynamics. For further details see Perez (2005).

7.1.1. Parameter variation and the RHP zero

With the importance of the location of the RHP zero, it is essential to know the variation of its location as a function of various parameters of the ship. Using model and data from Blanke and Christensen (1993), Figure 10, shows the change of the location of both the RHP zero and the LHP pole/zeroes of (56) when ship speed is changed. The nominal location of the poles and zeros are indicated by an "o" in the Figure. The RHP variation is significant with ship speed and also with vertical location of the meta-centre (restoring term). The latter will change with the loading condition and trim of the vessel.

7.1.2. Achievable damping

While the RHP zero is limiting the maximal achievable rudder roll damping, actual achievable damping is determined by the magnitude of the sensitivity function $S(j\omega)$ in Eq. (35), which

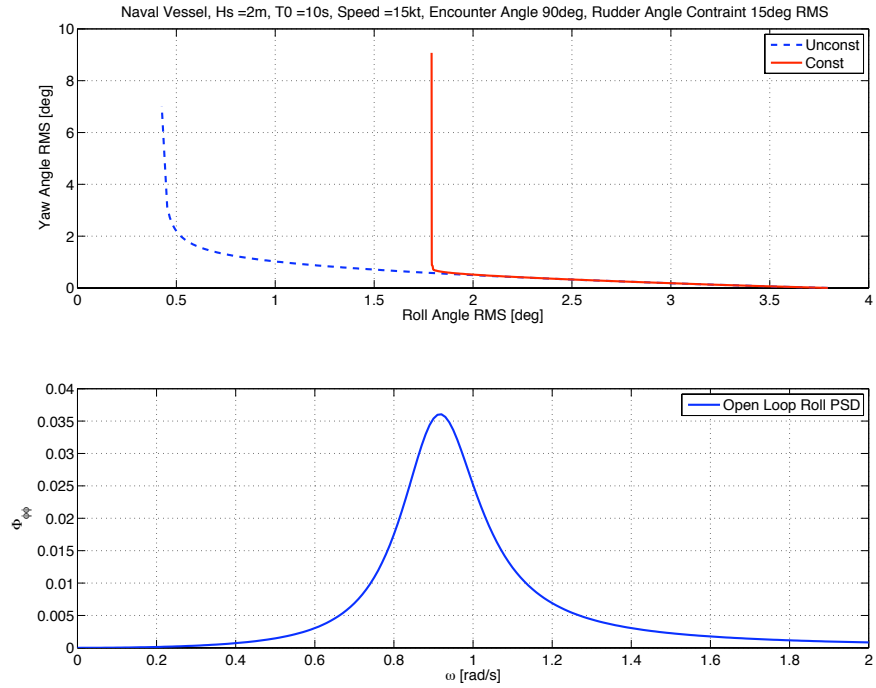

Figure 9: Example of performance limitations bounds and roll reduction *vs* yaw interference for a give sea state.

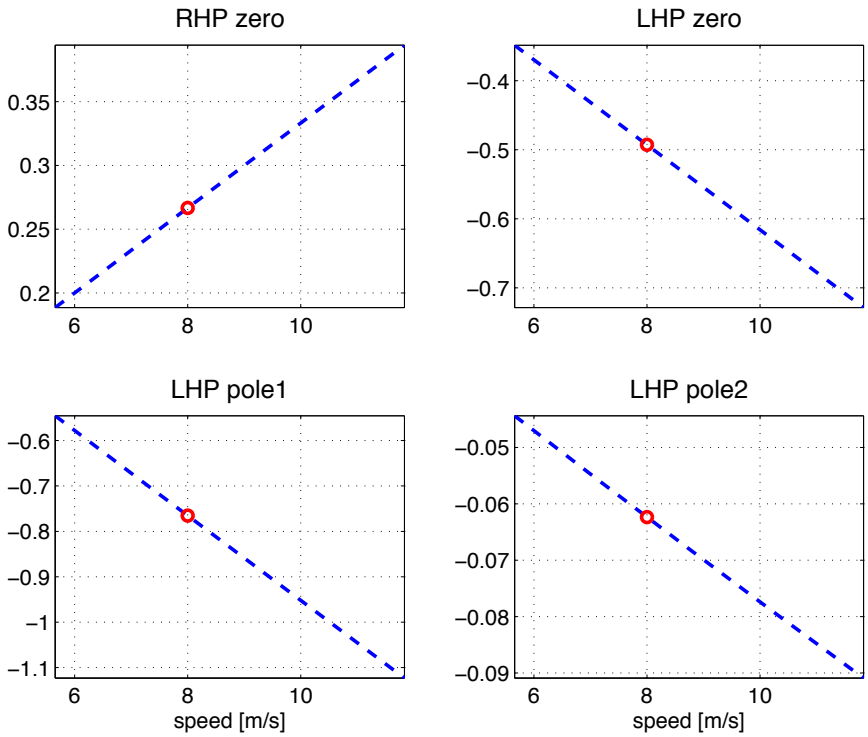

Figure 10: Change of poles and zeros with ship speed.

also depends of the remaining dynamics. A controller that achieves the minimal variance in roll in closed loop was derived in Perez et al. (2003). Given a motion spectrum $\Phi_{\phi\phi}(\omega)$ with a spectral factorisation

$$\Phi_{\phi_{ol}\phi_{ol}}(\omega) = H_d^*(j\omega)H_d(j\omega), \tag{63}$$

define a modified rudder to roll transfer function with the right half plane zero mirrored to the left half plane

$$G_{\phi\delta}^-(s) = G_{\phi\delta}(s)\frac{s+q}{s-q}. \tag{64}$$

Determine also the stable part of the product

$$H_d(s)\frac{s+q}{s-q} = \sum_{p_i<0}\frac{a_i}{1+\frac{s}{p_i}} + \sum_{p_j\geq 0}\frac{a_j}{1+\frac{s}{p_j}} \tag{65}$$

$$= H_d^-(s) + H_d^+(s). \tag{66}$$

Then the best achievable roll damping is obtained by the controller (Perez (2005))

$$
\begin{aligned}
Q(s) &= (H_d(s)G^-_{\phi\delta}(s))^{-1}H^-_d(s) && (67)\\
C_{\delta\phi}(s) &= (1 - G_{\phi\delta}(s)Q(s))^{-1}Q(s) && (68)\\
RR_{opt}(s) &= G(s)Q(s) && (69)\\
&= H_d^{-1}H_d^- \frac{s-q}{s+q} && (70)
\end{aligned}
$$

Inserting in the expressions for $Q(s)$ into $C_{\delta\phi}(s)$ gives

$$C_{\delta\phi}(s) = (G^-)^{-1}(1 - \frac{s-q}{s+q}H_d^{-1}H_d^-)^{-1}(H_d^{-1}H_d^-), \tag{71}$$

This controller is stable but non-causal. A realizably sub-optimal control could be obtained by padding necessary poles on the controller. The controller shows a strong dependency with the wave-induced roll motion spectra and also the variations of the rudder to roll transfer function parameters due to changes in vessel speed. Therefore, this controller is not practical without the exact form of the $H_d^{-1}H_d^-$ and parameter adaptation for $G_{\phi\delta}(s)$.

As an illustration, if

$$H_d(s) = \frac{\omega_w^2}{s^2 + 2\zeta_w\omega_w s + \omega_w^2}, \tag{72}$$

then

$$H_d^-(s) = -\frac{sa + b}{s^2 + 2\zeta_w\omega_w s + \omega_w^2}, \tag{73}$$

with parameters

$$
\begin{aligned}
b &= \omega_w^2 \frac{-\omega_w^2 + 2q\zeta_w\omega_w + q^2}{\omega_w^2 + 2q\zeta_w\omega_w + q^2} && (74)\\
a &= \frac{2q\omega_w^2}{\omega_w^2 + 2q\zeta_w\omega_w + q^2}. && (75)
\end{aligned}
$$

Hence, the product $H_d^{-1}H_d^- = as + b\omega_w^{-2}$ and the theoretical result for roll reduction

$$RR = \frac{as + b}{\omega_w^2}\frac{s-q}{s+q}, \tag{76}$$

which would be optimal for the wave model specified, but not obtainable. This is an alternative formulation the constraint (62) for the specific spectral factor (72).

7.2. Design from Sensitivity Specification

Given the integral constraints on the sensitivity, one can opt for calculating the controller directly from a specification of desired sensitivity function $S(\omega)$. The form of the sensitivity function for roll damping should asymptotically approach one at high and very low frequencies whilst satisfying the Poisson integral constraint (40). Attempting to reduce roll at high frequencies is impossible, reducing at very low frequencies would prevent the natural heel required

during a turn of a ship and would deteriorate manoeuvring capability. Damping should be high in the frequency range of sea-induced motion. A desired sensitivity function candidate can be

$$S_d(s) = \frac{\frac{s^2}{\omega_d^2} + 2\zeta_d \frac{s}{\omega_d} + 1}{(1 + \frac{s}{\beta\omega_d})(1 + \frac{\beta s}{\omega_d})}. \tag{77}$$

This sensitivity will not be realisable since it does not satisfy the integral constraint (40). The fundamental aspect of the above sensitivity is the size and location of the notch effect, which will be approximated by the true sensitivity. However, the side-lobes of the true sensitivity leading roll amplification will be imposed by the integral constraint (40).

With control action (rudder angle) $\delta(s) = C_{\delta\phi}(s)\phi(s)$ the sensitivity to roll motion disturbance is

$$S(s) = (1 + C_{\delta\phi}(s)G_{\phi\delta}(s))^{-1} \tag{78}$$

The stable and causal controller required to obtain a desired specification is

$$C^s_{\delta\phi}(s) = (S_d(s)^{-1} - 1)G^{-1}_{\phi\delta(s)} \frac{1 - \frac{s}{q}}{1 + \frac{s}{q}} P(s)^{-1} \tag{79}$$

where $P(s)$ is a polynomium comprising any poles needed for realizability of $C^s_{\delta\phi}(s)$. The specification obtainable is then

$$S_{obtained}(s)^{-1} = 1 + (S_d(s)^{-1} - 1)\frac{1 - \frac{s}{q}}{1 + \frac{s}{q}} P(s)^{-1} \tag{80}$$

This controller that follows from the specification (77) and the linear rudder to roll dynamics (56), takes the form

$$C^s_{\delta\phi}(s) = \frac{sk_1}{c_{\phi\delta}\omega_d} \frac{\frac{s^2}{\omega_p^2} + 2\zeta_p \frac{s}{\omega_p} + 1}{\frac{s^2}{\omega_d^2} + 2\zeta_d \frac{s}{\omega_d} + 1} \frac{(1 + s\tau_{p1})(1 + s\tau_{p2})}{(1 + s\tau_{z1})(1 + \frac{s}{q})}, \tag{81}$$

where $k_1 = (\beta + \beta^{-1} - 2\zeta_d)$ and $P(s) = 1$. This controller is a feedback from roll rate and is hence realisable. The bi-quadratic part of controller with complex poles given by the zeros of the specification and complex zeros given by the poles of the roll dynamics of the vessel, was suggested in Blanke et al. (2000a), where ability was demonstrated to tune to variations in roll motion spectra met in costal areas in Denmark. The main tuning parameter is ω_d and tuning is easily achieved to different sea conditions, on the condition that there is a separation of around a factor 3 or more between the ω_d and the RHP zero, at q. This separation is needed in order to avoid a large water-bed effect if form of undesired amplification of roll disturbances at frequencies below the range where damping is achieved. In practice, waterbed caused amplification beyond 1.2 to1.3 rad/s would be undesirable. Figure 11 shows the sensitivity function calculated from an identified dynamic model of a Danish SF300 vessel. The RHP zero at the medium speed condition was identified to be $q = 0.18$ rad/s. To cope with changes in the roll disturbance spectrum, a bank of 4 controllers were implemented, which the pilot can selected according to the dominant roll period.

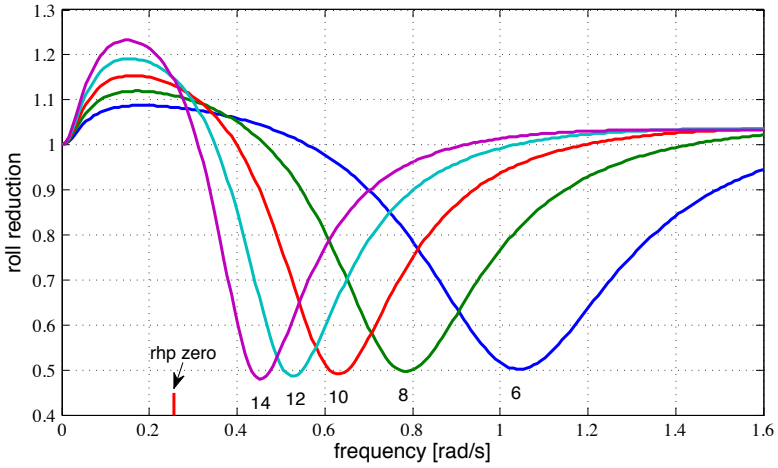

Figure 11: Specification driven design in with different tunings of the parameter $2\pi/\omega_d$ (6, 8, 10, 12, 14 sec). Vessel data are Blanke and Christensen (1993) at nominal speed $8m/s$ and displacement $450m^3$. The right half plane zero is at 0.26 rad/s is rather close to the range where damping is required.

7.3. Performance at Sea

The performance of this control scheme for combined heading control and rudder-roll damping is shown in Figures 12 and 13. Figure 12 shows a condition of quartering seas and ship speed in the 18-20 kt range. The RRD part of the algorithm is toggled between *off* and *on* every 10 minutes. Longer test sequences (15-18 min) could be of benefit to reduce statistical variation of waves but longer tests were not possible in this test due to non-stationarity of the sea, influenced by cost and wave patterns from shallow water around islands. Figure 13 show the power spectra of the middle two of the four tests in the sequence.

Achieved roll damping is estimated from a model that compensates for development in weather, $\sigma_\varphi = (t_0 + \alpha_t t_i)(1 + \alpha_{rrd}\mathbf{1}_{rrd})$ where σ_φ is observed standard deviation of roll angle, α_t accounts for development in external conditions, t_i is time elapsed by end of test i, α_{rrd} is the achieved roll damping of the test and $\mathbf{1}_{rrd}$ is 1 for RRD *on* and 0 otherwise. This test shows an achieved roll damping of 49%. The plot of motion spectra in Figure 13 clearly illustrate and confirm the theoretical sensitivity function from Figure 11.

8. Evolution of Roll Damping Control using Fins and Rudder

The control methods employed for roll damping have evolved over several decades but with jumps in the theoretical understanding of performance bounds described above. When new control theory has emerged, it has soon found its way to the marine field and also the roll damping control problem has been pursued.

8.1. Evolution of Rudder Roll Damping Control

The first full-scale trials of Rudder Roll Damping (RRD) are believe to have been conducted by van Gunsteren (1974) in the motor yacht *M.S. Peggy* in The Netherlands. The controller used

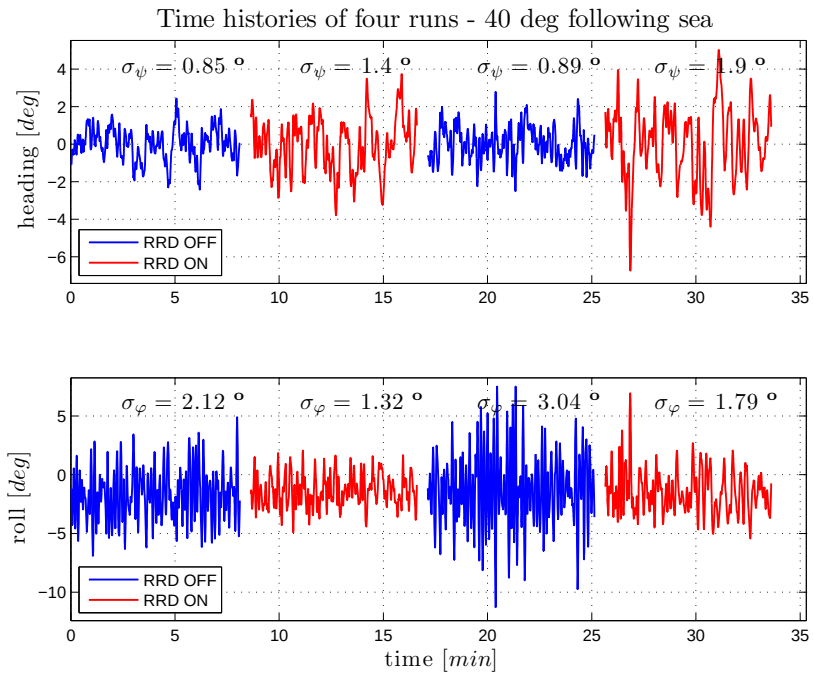

Figure 12: Time histories of a sequence with RRD toggled between *off* and *on*. Sea condition is quartering sea (40 deg from aft) and ship speed around 15 kt. The measured RRD efficiency is 49%.

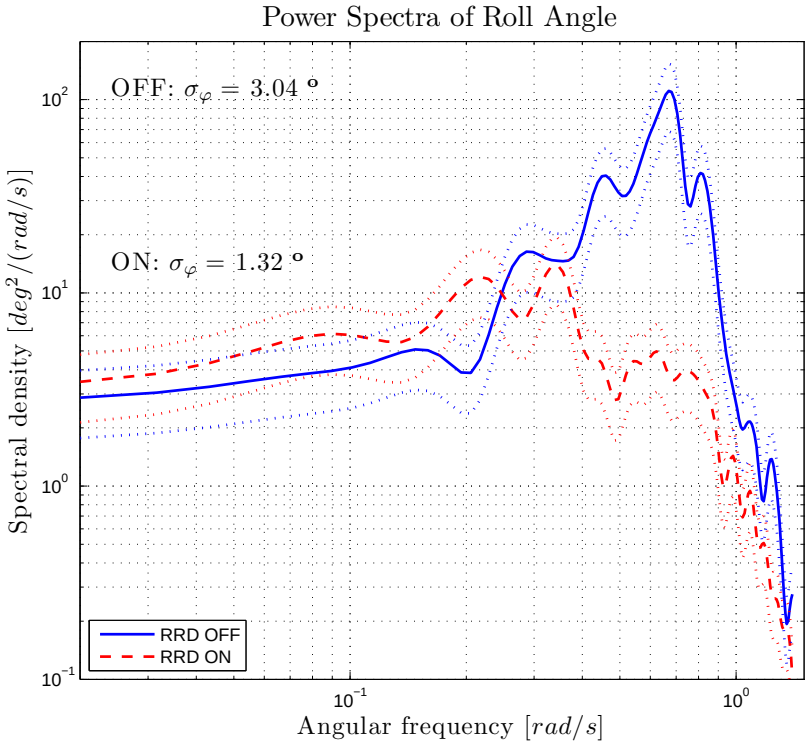

Figure 13: Power spectra of the sequences two and three in Fig. 12 with 1 σ uncertainty bounds are shown in dotted lines.

was a proportional controller that used roll rate and also to yaw angle and rate. During the trials, a roll reduction of 43% DSA[1] was obtained.

Cowley and Lambert (1972) presented a study of rudder roll stabilisation in which they used an analog computer model and a scale model of a fast container ship to test the hypothesis that a rudder could be used as a stabilising device. The controller used consisted of an autopilot and a roll feedback loop. The autopilot was a phase-lead compensator designed without considering the effect of roll motion. The roll loop was added after the autopilot was designed; this consisted of a simple gain feedback loop with roll angle. In the scale-model tests, the model was constrained in yaw and sway, and a moving weight was used to simulate an irregular beam sea. The continuation of this work was reported in Cowley (1974). In this work, a free-running scale model was used first then followed by full-scale sea trials. Model tests in irregular quartering seas gave a roll reduction of 50% DSA. Sea trials on a container ship gave reductions of 20% in moderate seas. The results of further full scale trials were reported in Cowley and Lambert (1975). The data were taken from seven Transatlantic crossings of a container ship fitted with a RRD system. The average roll reduction was of 40% DSA. Motivated by these results, RRD was further explored within the naval environment in the United Kingdom. The first of these results were reported by Carley (1975) and Lloyd (1975a). Neither of them envisaged a successful application of RRD for navy vessels. Carley (1975) provided the first feasibility analysis on the use of rudder as a stabiliser. This was a theoretical study based on models obtained from data of sea trials. In this study, he not only looked at the potential of the rudder to induce roll, but also the consequences for the steering characteristics of the vessel. The transfer functions from rudder to roll and to heading, $G_{\phi\delta}(s)$ and $G_{\psi\delta}(s)$, were estimated using system identification, and the following controllers were used:

$$C_\psi(s) = K_1 \frac{1 + aT_1 s}{1 + T_1 s} + \frac{1}{T_3 s}, \qquad C_\phi(s) = K_2 \frac{s(1 + T_1 s)}{s^2 + 2\xi\omega_\phi s + \omega_\phi^2},$$

where ω_ϕ in the roll controller is the natural roll frequency of the vessel and the last term of the heading controller (autopilot) is an optional weather-helm term. Using the above controllers, Carley (1975) investigated issues related to the stability of the closed-loop system and the coupling between roll and heading and frequencies at which roll reduction could be achieved. This was done using the sensitivity transfer functions. This study recognised the limitation imposed on the control system design due to the non-minimum phase characteristics of the rudder-to-roll response with the possibility of roll amplification at low encounter frequencies, and the trade-off between roll reduction and heading interference.

Lloyd (1975a) presented data from trials of a frigate, which show that forced roll induced by rudders (in calm water) is similar in magnitude to that induced by fins. He also presented a mathematical model, and simulation results for rudder stabilisation that compared the roll power spectral densities for the stabilised and unstabilised ship. The controllers used were similar to those used by Carley, as shown above. The highest roll reduction obtained was 40%, and this was for a simulated sailing condition of 60 deg encounter angle (quartering seas). The work was concluded with remarks similar to those made by Carley (1975) regarding the limitations due to the roll amplification at low frequencies.

The research in US also started in the mid 1970s. In 1974, the David Taylor Naval Ship Research and Development Center (DTNSRDC) started investigations on the use of RRD for

[1]Double significant amplitude is average of the largest one-third roll peak-to-trough amplitudes.

the US Navy (USN). In 1975, it was concluded that not all the classes had the necessary rudder-induced roll moment necessary for achieving good performance (Baitis et al., 1983). At this time, US Coast Guard (USCG) *Hamilton* cutter class was undergoing trials to improve the helicopter-vessel interaction. These trials showed that roll stabilisation was an important factor in performance and safety of helicopter landing and take-off. Since anti-roll tanks and fin stabilisers were not an economically viable alternative, a joint USN-USCG RRD research program was started in 1975. Two prototype vessels from the USCG *Hamilton* class went for trials with a RRS in 1979. The results of these trials were reported by Baitis (1980) and Baitis et al. (1983). These trials went further with regards to the evaluation of ship performance under rudder roll damping; they assessed not only the roll reduction and heading interference, but also the increase in ship operability with different controllers. The roll reductions reported were between 31% and 49% for beam seas, about 22% in bow seas and 28% in quartering seas. The control scheme used a roll-rate gain loop which was added to the manual control provided by the helmsman. The addition of a roll-angle gain loop was also attempted and it proved to increase performance only in quartering seas. It was concluded that unless the controller could alter the loop signals used for feedback, it was best to use roll-rate feedback. This work also evaluated the limitations imposed by the rudder rate. Tests with the original rudder rate of 4.7 deg/s and a modified 21 deg/s were performed. It was shown that the limited authority of the rudder machinery, leading to the rudder inability to follow the commanded angle, provided significant degradation in performance; and hence, constrained control should be used. The comment was also made that adaptivity with respect to sailing conditions was desirable.

During the 1980s, there was a significant contribution to the problem of RRD due to the work of different research groups which targeted the development in different countries: The Netherlands, Denmark, and Sweden. One of the most significant contributions to the developments of RRD was done by Dutch researchers. This was the result of a cooperative project between Delft University and the Royal Netherlands Navy, which started in 1981. This research evolved from computer simulations, to scale-model trials and finally to full scale trials performed in 1983. Most of the work has been reported by van der Klugt (1987), and also by van Amerongen et al. (1990). The control design was made using LQG techniques without considering the limitations imposed by the actuators, and then the design was modified so as to deal with these nonlinearities. The state vector considered was $[v', p, r, \phi, \psi]^T$, where v' is the sway velocity due to the rudder action only. Three methods were tested to avoid saturation of the steering machinery: gain scheduling, automatic gain control (AGC), and adaptive criterion. The hill-climbing technique was used to compute the sets of gains for different frequencies and intensities of the wave-induced forces. These gain sets were then used in a gain scheduling control scheme. The characteristics of the disturbance were estimated using Kalman filters and this was used to change the gains. This control approach performed well in simulations, but its performance fell short of expectations during full-scale trials. In addition, it did not guarantee that saturation of the steering machinery would not occur. The second method used AGC to limit the action demanded from the steering machinery. This AGC system would reduce the control command to ensure that saturation never occurs (the philosophy is similar to that of antiwind-up use in PID controllers). The main advantage of this is the prevention of phase lag induced by rate limitations, which could lead to closed-loop stability problems.

The final proposal of the Dutch group was an adaptive scheme to change the weighting coefficients in the cost function used for the LQG problem. By applying appropriate filtering, a frequency separation was obtained, and total rudder angle was separated into two components: $\delta_c = \delta_\phi + \delta_\psi$. These two components were obtained by solving two LQG problems; that is, the

total cost was of the form

$$J = \lambda_\phi J_\phi + J_\psi,$$

where

$$J_\phi = q_p\, var[p] + q_\phi\, var[\phi] + var[\alpha_\phi],$$

and

$$J_\psi = q_\psi\, var[\delta\psi] + var[\alpha_\psi],$$

with the variances interpreted as

$$var[y] = E[y^2] \approx \lim_{T\to\infty} \frac{1}{T} \int_0^T y^2(t)\, dt.$$

The parameters q_i were fixed, and the parameter λ_ϕ, was adapted online based on speed, maximum rudder angle allowed, max rudder rate, max heading deviations, *etc*. This adaptation is done slowly, and once a new λ_ϕ is obtained, the Ricatti equations associated with the LQR problem are solved online using a state-space representation based on the innovations model. The control law was of the of the form

$$\delta_c = \mathbf{K}_\phi \cdot [v', p, \phi]^T + \mathbf{K}_\psi \cdot [r, \delta\psi]^T.$$

Full-scale trials with the gain scheduling scheme combined with the AGC gave roll reductions of up to 65% for conditions in which the encounter frequency was close to the roll natural frequency. However, at higher and low encounter frequencies, the performance deteriorated as expected.

The Royal Danish Navy introduced RRD on the SF300 vessels, which are relatively fast monohull patrol vessels. These vessels have three rudders and three propellers, and the two wing rudders are used for RRD. The development was a collaboration between the Navy and a private shipyard. The results of some tests were presented by Blanke et al. (1989). The controllers were designed using LQG techniques considering a single multi-variable system. Investigation into the possibility of decoupling the roll from the yaw for control design led to the conclusion that this was not viable for these vessels. An adjustment was introduced for the operator to decide on roll reduction vs. heading interference. On the one extreme, the control objective was only to keep the course, while on the other, it was only to reduce the roll. It was noticed that when sailing at low speeds, the control command could saturate the steering machinery, leading to phase lags between the desired rudder angle and that achieved—which decreased the performance. To address this issue, an AGC mechanism was used. Regarding filtering, the yaw signal was filtered with a nonlinear high-gain observer to eliminate the wave frequency so only the low-frequency components were used as a heading feedback signal for the autopilot. For the roll angle and rate signals, the filtering was kept to a minimum to avoid delays which could affect the performance. The performance reported during initial tests for moderate sea states was in the range of 50–60% for beam and quartering seas and between 35–40% for quartering seas. However, further work on these vessels was reported by Blanke et al. (2000b), due to the lower performance recorded during operations. The SF300 is a multi-role naval vessel; and as such, significant variations in the loading conditions can be expected for the different missions performed by the vessel. This, in addition to a motion spectra different than those anticipated during the control system design, resulted in a performance lower than expected. Experience from data collected on operations in inner Danish waters showed that the wave spectra can have a significant spreading and more energy at low frequency than the idealised spectra commonly

used for design in naval architecture. The $\mathcal{H}_\infty$ approach was then taken. The desired rudder angle was separated into two components $\delta_d = \delta_\phi + \delta_\psi$, where

$$\delta_\phi = k_r\, u_{rel} \frac{s^2 + 2\xi_z \omega_z s + \omega_z^2}{s^2 + 2\xi_p \omega_p s + \omega_p^2} (\tau_p p(s) + \tilde{\phi}(s)),$$

where $\tilde{\phi}$ was the high-pass filtered roll angle. The autopilot control was nonlinear with appropriate gain scheduling according to the speed of the vessel and the thrust of the propulsion devices:

$$\alpha_\psi = f(r, \delta\psi, u),$$

see Blanke et al. (2000b) for further details. The final control design objective was to achieve 50% reduction in most sailing conditions and for the speed envelope of the operations performed by the vessels. Because of the widely varying conditions, the controller could be switched manually according to the wave period estimated by the operator: 6 s, 8 s, 10 s, 12 s and 14 s. The resulting sensitivity frequency response functions were shown in Figure 11 and performance at sea shown in Figures 12 and 13.

Källström et al. (1988), reported the implementation of RRD on ships of the Royal Swedish Navy. The system evolved into a commercial product called ROLL-NIX. This system was designed for use on straight courses; it switched off automatically when major manoeuvring was required, and back on when the vessel resumed a steady course. This ensured no interference with manoeuvring in situations requiring rapid course changes. The control algorithm was based on LQG, and incorporated adaptation mechanisms to cope with different weather conditions. During 1987, two types of vessels from the RSN were fitted with ROLL-NIX. These were a fast attack craft (35 m long, 170 m^3 of displacement) and mine layers (100 m long, 3300 m^3). The performance of the attack craft was in the range of 45–60% for beam and quartering seas in weather conditions of 4, 5 and 6 Beaufort scale at a speed of 27 kt. The results on the mine layer *HMS Carlskrona* was in the range of 40–45% for beam and quartering seas in weather conditions of 4 Beaufort scale at the speed of 16 kt.

8.2. Control theoretic approaches

During the 1990s, there was significant research activity on the theoretical aspects of the RRD control problem. In particular, the robustness properties of the controller and adaptive techniques gained much attention. Several different control techniques were proposed, but only a few full-scale implementations were reported.

8.2.1. Sensitivity and robustness issues

Blanke and Christensen (1993) studied the sensitivity of the performance of linear quadratic (LQ) optimal control to variations in the coupling coefficients of the ship equations of motion. They used a linear model based on the hydrodynamic data estimated during the design stage of the SF300 vessels. Using a simple multi-variable LQ controller, they defined a nominal design, and analysed the changes in performance due to changes in the following parameters of the model: U—speed; K_p—roll moment due to roll rate; N_p—yaw moment due to roll rate; and VCG—vertical centre of gravity. It was found that small changes in these parameters can modify the dynamic response of a vessel significantly. Further work based on sea trials of sister ships with modifications in the appendages and different load conditions was reported by Blanke (1996). It was found that the influence of the linear roll damping coefficient N_p was quite significant. In this work, a model for structured uncertainty was also proposed.

8.2.2. Linear Quadratic (LQ) optimal control

Zhou et al. (1990), proposed the use of recursive prediction error methods to identify the rudder to motion response and combine this with a Linear Quadratic Gaussian (LQG) controller. Katebi et al. (1987), also proposed the use of LQG. A main issue with optimal control approaches is that optimal is optimal according to which criterion is specified. A quadratic criterion expressed as

$$\begin{aligned} J &= \int_0^\infty (\mathbf{x}^T(t)\mathbf{R}\mathbf{x}(t) + \mathbf{u}^T(t)\mathbf{Q}\mathbf{u}(t))dt \qquad (82) \\ \text{subject to:} & \\ \dot{\mathbf{x}}(t) &= \mathbf{A}\mathbf{x}(t) + \mathbf{B}\mathbf{u}(t) \\ \mathbf{y}(t) &= \mathbf{C}(t)\mathbf{x}(t) \\ \mathbf{x}(t=0) &= \mathbf{x}_0 \end{aligned}$$

or the equivalent quadratic optimal problem formulated in the frequency domain, or formulated in discrete time, all have the design issue that the wave suppression specification is not part of the design setup, unless the system dynamic model includes a model of the wave disturbance. Including wave dynamics in the system model means that wave dynamics need be identified since the optimal control solution includes the **A** matrix, or transfer functions that include the equivalent dynamics, in the calculation of the feedback control. In an LQG state space solution, where feedback from estimated state is required, this dynamics is included in the Kalman filter or the state observer, which provides state estimation. If not included, the controller will increase the damping of the ships roll at the natural roll frequency, but since roll motion is a consequence of the combined sea disturbance and the response operator of the ship, significant roll motion energy is commonly found outside the region of natural roll and disturbance rejection of the control is adequate only if the disturbance spectrum is accounted for.

When state feedback is employed feedback from the roll angle should be avoided for two reasons. One is that natural heel due to ballasting or wind should not be attempted compensated by rudder or fins. Another that a ship needs to heel in order to rapidly change its course and roll damping should not counteract heading alteration capabilities of a vessel. The solution is to use roll-rate feedback or equivalently, in terms of classical controllers, use a high-pass filter on the roll angle as part of the feedback loop.

8.2.3. Quantitative Feedback theory

The Quantitative Feedback Theory (QFT) (Horowitz and Sidi, 1978; Horowitz, 1991) is a technique to obtain robustness where model uncertainty is mapped into the complex Nyquist ($\varphi - dB$) plane and computer assisted design shapes the controller frequency response such that desired properties in the Nyquist plane are obtained despite the uncertainties. The QFT design was investigated in Hearns and Blanke (1997) and Hearns and Blanke (1998c) to design cascade SISO controllers for roll and yaw which targeted the problem of uncertainty in the model.

8.2.4. $\mathcal{H}_\infty$ optimal control

Changing the optimisation criterion from quadratic norm to a maximum norm in the $\mathcal{H}_\infty$ optimal control gives a setop for design where output sensitivity is directly specified. The optimisation criterion for a combined roll damping and heading control would read

$$\left\| \begin{matrix} W_{\varphi\varphi}(\omega)S_{\varphi\varphi}(\omega) \\ W_{\psi\psi}(\omega))S_{\psi\psi}(\omega) \end{matrix} \right\| \leq \gamma_1 \qquad (83)$$

where $W_{\varphi\varphi}$ and $W_{\psi\psi}$ are weighting functions and $S_{\varphi\varphi}$ and $S_{\psi\psi}(\omega)$ closed loop sensitivity against output disturbances in roll and heading, respectively. $\gamma_1 \geq 1$ is a positive real number that approaches 1 for an optimal solution. Choosing a weighting for roll $W_{\varphi\varphi} = S_d^{-1}(\omega)$, see Eq. 77, will give a design with a trade-off between damping as desired and water-bed effect amplification if the system has a RHP zero, as is the case for rudder used as actuator but also could be so for fin solution, depending on the position of the fins. Grimble et al. (1993) used this approach for fin and combined fin-rudder control, as did Roberts et al. (1997). The specification $W_{\varphi\varphi}$ in the $\mathcal{H}_\infty$ optimisation gives results similar to the specification driven sensitivity design in Section 7.2, but the order of $\mathcal{H}_\infty$ controllers are high, being the sum of orders of the control object and of the weighting functions. Implementation and tuning concerns hence require model reduction of the controller. The weight function $W_{\psi\psi}(\omega)$) can be used to avoid that the controller attempts to control the heel angle.

8.2.5. Other $\mathcal{H}_\infty$ approaches

Stoustrup et al. (1995) and Sharif et al. (1994) compared the performance of $\mathcal{H}_\infty$ controller with that of an LQ controller, and found that for the former, the roll angle amplification at low frequencies is less than that for an LQ controller using feedback from both roll angle and roll rate. Stoustrup et al. (1995) also studied the coupling between roll and yaw and used a specification on allowed yaw amplification to achieve a controller through a Youla-Kučera parametrisation of the controller. Yang and Blanke (1998) incorporated the uncertainty models—proposed by Blanke (1996)—into the robust control design framework, and used μ-synthesis.

8.2.6. Sliding mode nonlinear control

Laudval and Fossen (1997) took the nonlinear approach and proposed the use of sliding mode control. This is, perhaps, the only reference in the literature that uses a nonlinear model for the design. The main reason for the adoption of linear models is that RRD is mostly used in course-keeping operations, and thus, only small deviations from the steady-state course should be expected.

8.2.7. Autoregressive stochastic control

A stochastic approach based on autoregressive models was proposed by Oda et al. (1992) and Sasaki et al. (1992). A multi-variable autoregressive model

$$\mathbf{y}(k) = \sum_{j=1}^{N} \mathbf{A}(j)\mathbf{x}(k-j) + \sum_{j=1}^{N} \mathbf{B}(j)\mathbf{u}(k-j) + \mathbf{v}(k) \tag{84}$$

was fitted to data where $\mathbf{y}$ are measurements, e.g. roll and heading, $\mathbf{u}$ is input, here rudder angle, and $\mathbf{v}$ is noise. The model was identified from data collected in calm water, and then an LQ optimal control problem was solved to obtain the control gains. The modelling and control design of this approach fall into the framework of Generalised Predictive Control (GPC), which can be reduced to an LQG problem. In order to avoid the saturation of the steering machinery, the cost function minimised included a term that penalised the rate of rudder motion. Full-scale implementations were reported by Oda et al. (1996) and Oda et al. (1997). Later work using this approach included also fins as actuators Oda et al. (2001)

8.3. Evolution of Fin and Combined Rudder and Fin Stabiliser Control

From the control system design point of view, the problem of control of fin stabilisers is relatively simpler than that of rudders stabilisers. The main reason for this is that the design can be performed by decoupling the roll from the other equations of motion; and, in general, the non-minimum phase dynamics do not affect the design—NMP dynamics appear only if the fins are located aft from the centre of gravity. Because of this, classical PID and $\mathcal{H}_\infty$ types of controllers usually perform well (Hickey et al., 1995, 1997, 1999; Hickey, 1999; Katebi et al., 2000), and most of the early literature on fin stabilisation focused strongly on the hydrodynamic aspects of the fins, fin size and location rather than control design (Allan, 1945; Conolly, 1969; Lloyd, 1972; Baitis et al., 1972; Lloyd, 1975b; Dallinga, 1993). This research continues to date due to tendency of fins to develop dynamic stall conditions in moderate to severe sea states Gaillarde (2002). This latter work has motivated the control strategy proposed in Perez (2005).

As mentioned above, the traditional approach for the design of fin stabilisers consists of using the decoupled roll motion equations. Despite this, Carley and Duberley (1972), observed that the cross-coupling between roll, sway and yaw often reduces the performance of the fins, and therefore if the system as a whole is to operate optimally, and integrated control for rudder and fin should be considered. This way, the autopilot action does not counteract the action of the fins with regards to roll. This together with the developments of RRD has motivated a wealth of research into the combined rudder-fin stabilisation.

The work on control of combined fin-rudder stabilisers has reported the use of PID controllers (Hickey, 1999; Crossland, 2000; Tanguy et al., 2003; Crossland, 2003), LQG controllers (Källström, 1981; Sgobbo and Parsons, 1999) and H_∞ (Grimble et al., 1993; Sharif et al., 1995, 1994, 1996; Roberts et al., 1997; Crossland, 2003; Tanguy et al., 2003). Perez and Goodwin (2008) proposed the use of constrained MPC as a natural extension of their work on RRD.

9. Gyrostabilisers

As discussed in Section 4, a gyrostabiliser consists of a one or more spinning masses rotating at a constant angular velocity ω_s—see Figure 6. These devices are located in on the hull in such a way that a gyroscopic torque produced by a gyrostabiliser on the vessel opposes the roll moment generated by the waves. The coupled vessel-roll and gyro model can be modelled as follows:

$$\dot{\phi} = p, \tag{85}$$

$$K_{\dot{p}}\,\dot{p} + K_p\,p + K_\phi\,\phi = K_w - nK_g\dot{\alpha}\cos\alpha \tag{86}$$

$$I_p\ddot{\alpha} + B_p\dot{\alpha} + C_p\sin\alpha = K_g\,p\cos\alpha + T_p \tag{87}$$

Equation (86) represents the roll dynamics, whereas equation (87) represents the dynamics of the gyrostabiliser about the precession axis, where α is the precession angle, n is the number of spinning masses I_p is inertia, B_p is the damping, and C_p is the restoring term of the gyro about the precession axis due to location of the gyro centre of mass relative to the precession axis (Arnold and Maunder, 1961). The use of twin counter spinning masses prevents gyroscopic coupling with other degrees of freedom. Hence, the control design for gyrostabilisers can be based on a linear single degree freedom model for roll.

The wave-induced roll moment K_w excites the roll. As the roll motion develops, the roll rate p induces a torque along the precession axis of the gyrostabiliser. As the precession angle

α develops, there is reaction torque done on the vessel that opposes the wave-induced moment. The later is the roll stabilising torque:

$$X_g \triangleq -nK_g\dot{\alpha}\cos\alpha \approx -nK_g\dot{\alpha}. \tag{88}$$

Note that this roll torque can only be controlled indirectly through the precession dynamics in (87) via the precession control torque T_p. In the analysis presented in this paper, it is assumed that the spin angular velocity ω_{spin} is constant; and thus the spin angular momentum $K_g = I_{spin}\,\omega_{spin}$ is constant.

The precession control torque T_p is used to control the gyro. As observed by Sperry (Chalmers, 1931), the intrinsic behaviour of the gyrostabiliser is to use roll rate to generate a roll torque. Hence, one could design a precession torque controller such that from the point of view of the vessel, the gyro behaves as damper, that is,

$$T_p : \dot{\alpha}\cos\alpha \approx \beta\, p, \quad \beta > 1, \tag{89}$$

Then the coupled equations (86) -(87) simplify to

$$\dot{\phi} = p, \tag{90}$$

$$K_{\dot{p}}\,\dot{p} + (K_p + nK_g\beta)\,p + K_\phi\,\phi = K_w. \tag{91}$$

Perez and Steinmann (2009) propose a control design based on gyro-precession information only

$$T_p = -K_{\dot{\alpha}}\,\dot{\alpha} - K_\alpha\alpha, \tag{92}$$

which achieves the above goal and ensure stability. With this controller, the precession rate to roll rate transfer function takes the form

$$G_{\alpha\phi}(s) = \frac{\dot{\alpha}(s)}{\dot{\phi}(s)} = \frac{K_g s}{I_g s^2 + (B_g + K_{\dot{\alpha}})s + (C_g + K_\alpha)}, \tag{93}$$

with the necessary and sufficient condition for its stability being $B_g + K_{\dot{\alpha}} > 0$ and $C_g + K_\alpha > 0$. Since this transfer function is positive real, and the ship transfer function from roll moment to roll rate is also positive real, their feedback interconnections is passive and thus stable (Perez and Steinmann (2009)). Depending on how the precession torque is delivered, it may be necessary to constraint precession angle and rate. This is outside the scope of this paper.

10. Effect of Restoring Non-linearities and Parametric Resonance

The wave passage along the hull and the wave excited vertical motions result in variations of the vessel water-plane area, which is proportional to the roll restoring strength. These changes in the restoring terms coupled with a exchange of energy between roll and pitch can result in a rapid build up of roll angle for some vessels reaching angles up to 40 deg in just s few roll cycles. Figure 14 shows some experimental results of a container vessel experiencing this phenomenon (Holden et al., 2007). In a mathematical model, this physical effect can be described by a time-change in the roll restoring parameters; and therefore, the phenomenon is often described as roll parametric induced resonance, or simply parametric roll (Fossen and Nijmeijer (2012)).

The onset and the buildup of parametric roll requires the occurrence of concomitant conditions:

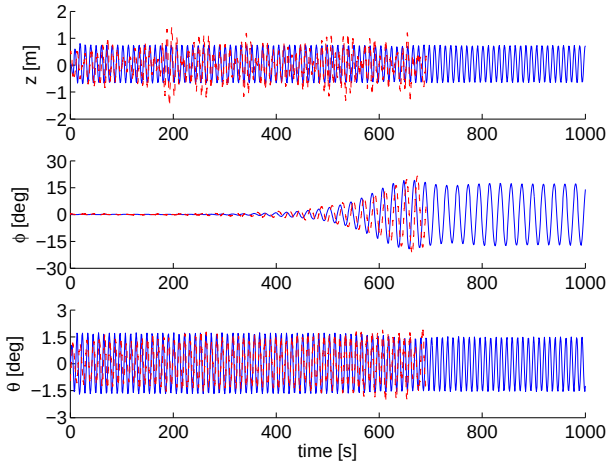

Figure 14: Experimental and model validation of a containership experiencing parametric roll while sailing in regular head seas. The experimental data for heave (z), roll (ϕ), and pitch (θ) is plotted in solid lines, whereas the model response is plotted in dashed lines.

- wave length is close to the ship length,
- encounter angles close to 0 or 180deg,
- encounter freq. close to twice the roll natural freq.,
- low roll damping,
- waves of certain height.

Different types of vessel have reported to experience parametric roll in head seas (encounter angles 180deg). Container carriers and fishing vessels, however, are the most prone to parametric roll. This is a consequence of modern hull designs with high bow flare and stern overhang, which result large variations in the intercepted water-plane area when a wave crest travels along the ship length.

In the last ten years parametric roll has attracted a significant research attention due to the millions of dollars lost every year in container cargo, and also the capsizing of fishing vessels. Mathematical models of different complexity have been proposed by the scientific community, most of them relying on the Mathieu Equation to describe the dynamics of the ship subject to parametric resonance. 1-DOF models considering the uncoupled roll motion have been widely used to analyse the critical phenomenon and derive stability conditions. Examples can be found in the papers by France et al. (2001) where the authors employed the 1-DOF roll equation to show that, in regular waves, this can be reduced to the Mathieu Equation in order to explain the onset of heavy roll motion in head seas. Santos Neves and Rodriguez (2006) proposed a 3DOF model coupling roll heave and pitch:

$$\mathbf{M}\,\ddot{\mathbf{q}} + \mathbf{D}(\dot{\mathbf{q}})\dot{\mathbf{q}} + \mathbf{g}(\mathbf{q},\zeta) = \boldsymbol{\tau}_w(\zeta,\dot{\zeta},\ddot{\zeta}), \tag{94}$$

where $\mathbf{q} = [z,\phi,\theta]^T$, and ζ is the wave elevation amidships. The restoring term $\mathbf{g}(\mathbf{q},\zeta)$ is a 3rd-order Taylor term (Holden et al., 2007) using scale-model experiments of a modern containership.

Damping of parametric resonance is in principle equivalent to that of damping of forced roll. The main challenge with parametric resonance is the amount of energy that is transferred through the resonance. If a resonance is allowed to develop to fully it may not be possible to stopped. Therefore, early detection of the phenomenon is crucial. Efforts have been made on the early detection of parametric roll by means of statistical testing of frequency synchronism between the peaks of roll and pitch motion (Galeazzi et al., 2009a, 2012). Results from simulation and experimental data indicate that the proposed tests can detect parametric roll as early as five roll cycles before the growth in roll is noticeable. Control schemes that increase roll damping via fin stabilisers have been proposed in Galeazzi et al. (2009b), and the use of anti-roll water tanks is considered in Holden et al. (2009). There has also been a proposal for control of vessel speed and heading so as to break the wave encounter frequency condition ($\omega_e = 2\omega_\phi$) (Breu and Fossen, 2010). The control of parametric roll resonance is still a topic of current research.

11. Conclusion and Research Outlook

In this paper, we have provided a tutorial and a large list of references on control aspects of roll motion control devices. These aspects include the type of mathematical models used to design and analyse the control problem, the inherent fundamental limitations and constraints that some of the designs may be subjected to, and how the performance of the controlled vessels is assessed. In the case of rudder roll damping, a formulation that allows one to assess the potential applicability of this technique was also revisited.

As a research outlook, one of the key issues in roll motion control is the adaptation to the changes in the environmental conditions. As the vessel changes speed and heading, or as the seas build up or abate, the dominant frequency range of the wave-induced forces can change significantly. Due to the fundamental limitations discussed in this paper, a non-adaptive controller may produce roll amplification rather than roll reduction. This topic has received some attention in the literature via multi-mode control switching, but further work in this area could be beneficial. Also on the topic of adaptation, some vessels use trim-flaps and interceptors to set the trim of the vessel, and they provide an opportunity for pitch and also roll control. The change in trim, affects the roll restoring coefficients, and therefore a shift in the vessel natural frequency in roll, which can affect the performance of the roll controller.

In the past recent years, new devices have appeared for stabilisation at zero speed, like flapping fins and rotating cylinders. Also the industry's interest in roll gyrostabilisers have been re-ignited. The investigation of control designs for these devices has not yet received much attention within the control community. Hence, it is expected that this will create a potential research activity.

In some sailing conditions, the wave passage along the hull and the wave excited vertical motions result in large variations of the roll restoring strength. These changes in the restoring terms coupled with a exchange of energy between roll and pitch can result in a rapid build up of roll for some vessels reaching angles up to 40^o in 5-10 roll cycles. In a mathematical model, this physical effect can be described by a time-change in the roll restoring parameters; and therefore, the phenomenon is often described as roll parametric resonance, or simply parametric roll. In the past 5 years, a significant attention has been put into early detection of this phenomenon, and some control proposals to reduce parametric roll are starting to appear in the literature. It is expected that this interesting non-linear problem will continue to be an area of intense research activity.

Acknowledgement

The permission of the Danish Navy to publish data from tests with the SF300 class and the close collaboration between J. Adrian and the second author are gratefully acknowledged.

References

Abkowitz, M., 1964. Lecture notes on ship hydrodynamics–steering and manoeuvrability. Tech. report hy-5, Hydro and Aerodynamics Laboratory Lyngby, Denmark.

Allan, J., 1945. Stabilisation of ships by activated fins. Transactions of The Royal Institution of Naval Architects RINA 87, 123–159.

Arnold, R., Maunder, L., 1961. Gyrodynamics and its Engineering Applications. Academic Press, New York and London.

Baitis, A., 1980. The development and evaluation of a rudder roll stabilization system for the WHEC Hamilton class. Tech. Rep. DDDTNSRDC/SPD-0930-02, DTNSRDC, Bethsada, MD.

Baitis, A., Cox, G., Woolaver, D., 1972. Evaluation of V active fin roll stabilisers. 3rd Ship Control System Symposium–SCSS, Bath, UK.

Baitis, E., Woollaver, D., Beck, T., 1983. Rudder roll stabilization of coast guard cutters and frigates. Naval Engineering Journal 95 (3), 267–282.

Blanke, M., 1981. Ship propulsion losses related to automatic steering and prime mover control. Ph.D. thesis, Servolaboratory, Technical University of Denmark.

Blanke, M., 1996. Uncertainty models for rudder roll damping control. In: Proc. of IFAC World Congress. Vol. Q. pp. 285–290.

Blanke, M., Adrian, J., Larsen, K., Bentsen, J., 2000a. Rudder roll damping in coastal region sea conditions. In: Proc. of 5th IFAC Conference on Manoeuvring and Control of Marine Craft, MCMC'2000.

Blanke, M., Adrian, J., Larsen, K., Bentsen, J., 2000b. Rudder roll damping in coastal region sea conditions. In: Proc. of 5th IFAC Conference on Manoeuvring and Control of Marine Craft, MCMC'2000.

Blanke, M., Christensen, A., 1993. Rudder roll damping autopilot robustness to sway-yaw-roll couplings. In: Proc. of 10th SCSS, Ottawa, Canada, 93–119.

Blanke, M., Haals, P., Andreasen, K. K., 1989. Rudder roll damping experience in Denmark. In: Proc. of IFAC workshop CAMS'89, Lyngby, Denmark.

Blanke, M., Knudsen, M., 2006. Efficient parametrization for grey-box model identification - a principal components approach. In: 14th IFAC Symposium on System Identification.

Breu, D., Fossen, T. I., 2010. Extremum seeking speed and heading control applied to parametric roll resonance. In: 8th IFAC Conference on Control Applications in Marine Systems, Rostock, Germany.

Carley, J., 1975. Feasibility study of steering and stabilising by rudder. 4rd Ship Control System Symposium–SCSS, The Netherlands.

Carley, J., Duberley, A., 1972. Design considerations for optimum ship motion. 3rd Ship Control System Symposium–SCSS, Bath, UK.

Chalmers, T., 1931. The Automatic Stabilisation of Ships. Chapman and Hall, London.

Conolly, J., 1969. Rolling and its stabilization by fins. Transactions of The Royal Institution of Naval Architects 111.

Cowley, W., 1974. Development of an autopilot to control yaw and roll. 3rd Ship Control System Symposium–SCSS, Bath, UK.

Cowley, W., Lambert, T., 1972. The use of a rudder as a roll stabiliser. 3rd Ship Control System Symposium–SCSS, Bath, UK.

Cowley, W., Lambert, T., 1975. Sea trials on a roll stabiliser using the ship's rudder. 4th Ship Control System Symposium–SCSS, The Netherlands.

Crossland, P., 2000. The effect of roll stabilization controllers on warship operational performance. In: 5th IFAC Conference on Manoeuvring and Control of Marine Craft MCMC'02. pp. 31–37.

Crossland, P., 2003. The effect of roll stabilization controllers on warship operational performance. Control Engineering Practice 11, 423–431.

Dallinga, R., 1993. Hydromechanic aspects of the design of fin stabilisers. Transactions of The Royal Institution of Naval Architects.

Fedyaevsky, K., Sobolev, G., 1964. Control and Stability in Ship Design. State Union Shipbuilding, Leningrad.

Fossen, T., 1994. Guidance and Control of Ocean Marine Vehicles. John Wiley and Sons Ltd, New York.

Fossen, T., 2002. Marine Control Systems: Guidance, Navigation and Control of Ships, Rigs and Underwater Vehicles. Marine Cybernetics, Trondheim.

Fossen, T. I., 2011. Handbook of Marine Craft Hydrodynamics and Motion Control. Wiley.

Fossen, T. I., Nijmeijer, H. (Eds.), 2012. Parametric Resonance in Dynamical Systems. Springer.
Frahm, H., 1911. Results of trials of anti-rolling tanks at sea. Trans. of the Institution of Naval Architects 53.
France, W., amd T. Treakle, M. L., Paulling, J., Michel, R., Moore, C., 2001. An investigation of headsea parametric rolling and its influence on container lashing systems. In SNAME Annual Meeting.
Freudenberg, J. S., Looze, D. P., 1985. Right half-plane poles and zeros and design trade-offs in feedback systems. IEEE Transactions on Automatic Control Engineering Practice AC-30, 555–565.
Freudenberg, J. S., Looze, D. P., 1988. Frequency Domain Properties of Scalar and Multivariable Feedback Systems. Springer Verlag New York.
Gaillarde, G., 2002. Dynamic behavior and operation limits of stabilizer fins. In: IMAM International Maritime Association of the Mediterranean, Creta, Greece.
Galeazzi, R., Blanke, M., Poulsen., N. K., 2009a. Parametric roll resonance detection using phase correlation and log-likelihood testing techniques. In: 8th IFAC International Conference on Manoeuvring and Control of Marine Craft, Guaruya, Brazil.
Galeazzi, R., Blanke, M., Poulsen, N. K., 2012. Early detection of parametric roll on ships. In: Fossen, T. I., Nijmeijer, H. (Eds.), Parametric Resonance in Dynamical Systems. Springer, Ch. 2.
Galeazzi, R., Holden, C., Blanke, M., Fossen., T. I., 2009b. Stabilisation of parametric roll resonance by combined speed and fin stabiliser control. In: 10th European Control Conference, Budapest, Hungary.
Gawad, A., Ragab, S., Nayfeh, A., Mook, D., 2001. Roll stabilization by anti-roll passive tanks. Ocean Engineering 28, 457–469.
Goodrich, G., 1969. Development and design of passive roll stabiliser. Trans. of The Royal Institution of Naval Architects, 81–88.
Grimble, M., Katebi, M., Zang, Y., 1993. $\mathcal{H}_\infty$–based ship fin-rudder roll stabilisation. In: 10th Ship Control System Symposium SCSS. Vol. 5. pp. 251–265.
Hearns, G., Blanke, M., 1997. Quantitative analysis and design of rudder roll damping controller. Technical Report R-1998-4243, Department of Control Engineering, Aalborg University, Denmark.
Hearns, G., Blanke, M., 1998a. Quantitative analysis and design of a rudder roll damping controller. In: Proc. IFAC CAMS'98.
Hearns, G., Blanke, M., 1998b. Quantitative analysis and design of a rudder roll damping controller. Tech. rep., Aalborg University.
Hearns, G., Blanke, M., 1998c. Quantitative analysis and design of rudder roll damping controllers. In: Proc. of CAMS'98.
Hickey, N., 1999. Control design for fin roll stabilisation. Ph.D. thesis, University of Strathclyde, Glasgow, UK.
Hickey, N., Grimble, M., Johnson, M., Katebi, M., Melville, R., 1997. Robust fin roll stabilisation of surface ships. In: Proc. of the 36th Conference on Decision and Control 1997, San Diego, California, USA.
Hickey, N., Grimble, M., Johnson, M., Katebi, M., Wood, D., 1995. $\mathcal{H}_\infty$ fin roll control system design. In: Proc. of IFAC Conference on Control Applications in Marine Systems, Tronheim, Norway.
Hickey, N., Johnson, M., Katebi, M., Grimble, M., 1999. PID controller optimisation for fin roll stailisation. In: Proc. of the International Conference on Control Applications, Hawai, USA.
Holden, C., Galeazzi, R., Fossen, T., Perez, T., 2009. Stabilisation of parametric roll resonance with active u-tanks via lyapunov control design. In: Proceedings of the European Control Conference 2009, Budapest, Hungary, August 23–26, 2009.
Holden, C., Galeazzi, R., Rodriguez, C., Perez, T., Fossen, T. I., Blanke, M., Neves, M. S., 2007. Nonlinear container ship model for the study of parametric roll resonance. Modeling, Identification and Control 28 (4), 87–103.
Horowitz, I., 1991. Survey of quantitative feedback theory (qft). Int. Journal of Control 53(2), 255–291.
Horowitz, I., Sidi, M., 1978. Optimum synthesis of non-minimum phase feedback systems with plant uncertainty. International Journal of Control 27(3), 361–386.
Källström, C., 1981. Control of yaw and roll by a rudder/fin stabilisation system. In: Proc. of 6th SCSS.
Källström, C., 1981. Control of yaw and roll by rudder/fin stabilization system. In: Proc. of 6th International Ship Control System Symposium (SCSS'81).
Källström, C., Wessel, P., Sjölander, S., 1988. Roll reduction by rudder control. In: Spring Meeting-STAR Symposium, 3rd IMSDC.
Katebi, M., D.D.K., W., Grimble, M., 1987. LQG autopilot and rudder roll stabilisation control system design. Proc. of the 8th ship Control System Symposium.
Katebi, M., Hickey, N., Grimble, M., 2000. Evaluation of fin roll stabilizer design. In: 5th IFAC Conference on Manoeuvring and Control of Marine Craft MCMC'00. pp. 31–37.
Lamb, H., 1932. Hydrodynamics, First edition piblished in 1879; Sixth edition published in 1932. First Cambridge University Press paper back edition published in 1993. Edition. Cambridge University Press.
Laudval, T., Fossen, T., 1997. Nonlinear rudder-roll damping of non-minimum phase ships using sliding mode control. Proc. of the European Control Conference, Brussel, Belgium.

Lewis, E. E., 1988a. Principles of Naval Architecture vol I: Stability and Strength, 3rd Edition. Society of Naval Architects and Marine Engineers, New York.

Lewis, E. E., 1988b. Principles of Naval Architecture vol III: Motions in Waves and Controllability, 3rd Edition. Society of Naval Architects and Marine Engineers, New York.

Lloyd, A., 1972. The hydordynamic performance of roll stabiliser fins. 3rd Ship Control System Symposium–SCSS, Bath, UK.

Lloyd, A., 1975a. Roll stabilisation by rudder. 4th Ship Control System Symposium–SCSS, The Netherlands.

Lloyd, A., 1975b. Roll stabiliser fins: A design procedure. Trans. of The Royal Institution of Naval Architects.

Lloyd, A., 1989. Seakeeping: Ship Behaviour in Rough Weather. Ellis Horwood.

Minorsky, N., 1935. Problems of anti-rolling stabilization of ships by the activated tank method. American Society of Naval Engineers 47.

Monk, K., 1988. A war ship roll criterion. Royal Institute of Naval Architects, 219–240.

NATO, 2000. Standarization Agreement: common procedures for seakeeping in the ship design process (STANAG) 3rd ed N0.4154. North Atlantic Treaty Organization (NATO), Military Agency for Standarization.

Norrbin, N., 1970. Theory and observation on the use of a mathematical model for ship manoeuvring in deep and confined waters. 8th Symposium on Naval Hydrodynamics, USA.

Ochi, M., 1998. Ocean Waves: The Stochastic Approach. Ocean Technology Series. Cambridge University Press.

Oda, H., Kanda, M., Hyodo, T., Nakamura, K., Fukushima, H., Iwamoto, S., Takeda, S., Ohtsu, K., 2001. The preliminary study of fin and rudder multivariate hybrid control system - advanced rudder roll stabilization system. In: Proc. CAMS'2001.

Oda, H., Ohtsu, K., Hotta, T., 1996. Statistical analysis and design of a rudder roll stabilization system. Control Engineering Practice 4 (3), 351—358.

Oda, H., Ohtsu, K., Hotta, T., 1997. A simulation study and full scale experiment of rudder roll stabilisation system. In Proc. of 11th Ship Control System Symposium SCSS, Southampton, U.K. 1, 299–313.

Oda, H., Sasaki, M., Seki, Y., Hotta, T., 1992. Rudder roll stabilisation control system through multivariable autoregressive model. In Proc. of IFAC Conference on Control Applications of Marine Systems–CAMS.

Perez, T., 2005. Ship Motion Control. Advances in Industrial Control. Springer-Verlag, London.

Perez, T., Fossen, T., 2007. Kinematic models for seakeeping and manoeuvring of marine vessels at zero and forward speed. Modeling Identification and Control, published by The Norwegian Society of Automatic Control. 28 (1).

Perez, T., Fossen, T., 2008a. Joint identification of infinite-frequency added mass and fluid-memory models of marine structures. Modeling Identification and Control, published by The Norwegian Society of Automatic Control. 29 (3).

Perez, T., Fossen, T. I., 2008b. Time-domain vs. frequency-domain identification of parametric radiation force models for marine structures at zero speed. Modeling Identification and Control, published by The Norwegian Society of Automatic Control. 29 (1), 1–19, doi:10.4173/mic.2008.3.2.

Perez, T., Goodwin, G., 2008. Constrained predictive control of ship fin stabilizers to prevent dynamic stall. Control Engineering Practice 16, 482–494.

Perez, T., Goodwin, G., Skelton, R., 2003. Analysis of performance and applicability of rudder-based stabilizers. In: Blanke, M., Ridao, P. (Eds.), Proc. $6^{t}h$ IFAC Symp. on Manoeuvring and Control of Marine Craft (MCMC'2003). Girona, Spain.

Perez, T., Revestido-Herrero, E., 2010. Damping structure selection in nonlinear ship manoeuvring models. In: 8th IFAC Conf. on Control Applications in Marine Systems, CAMS 2010, Rostock, Germany.

Perez, T., Steinmann, P., 2009. Analysis of ship roll gyrostabiliser control. In: 8th IFAC International Conference on Manoeuvring and Control of Marine Craft. September, Guaruja, Brazil.

Price, W., Bishop, R., 1974. Probabilistic Theory of Ship Dynamics. Chapman and Hall, London.

Roberts, G., Sharif, M., Sutton, R., Agarwal, A., 1997. Robust control methodology applied to the design of a combined steerign/stabiliser system for warships. IEE Proc. Control Theory Applications 144 (2), 128–136.

Roberts, G. N., 1993. A method to determine the applicability of rudder roll stabilization for ships. In Proc. of IFAC World Congress 5, 405–408.

Ross, A., June 2008. Nonlinear maneuvering model based on low-aspect ratio lift theory and lagrangian mechanics. Phd thesis., Dept. of Engineerign Cybernetics.

Santos Neves, M., Rodriguez, C. A., 2006. On unstable ship motions resulting from strong non-linear coupling. Ocean Engineering 33.

Sasaki, M., H. Oda, H., Seki, Y., Ohtsu, K., Hotta, T., 1992. Actual experiences in designing rudder roll control systems. In Proc. of IFAC Conference on Control Applications of Marine Systems–CAMS.

Schlick, O., 1904. Gyroscopic effects of flying weels on board ships. Transactions of The Institution of Naval Architects INA.

Sellars, F., Martin, J., 1992. Selection and evaluation of ship roll stabilization systems. Marine Technology, SNAME 29 (2), 84–101.

Serón, M., Braslavsky, J., Goodwin, G., 1997. Fundamental Limitations in Filtering and Control. Springer.

Sgobbo, J., Parsons, M., 1999. Rudder/fin roll stabilization of the USCG WMEC 901 class vessel. Marine Technology 36 (3), 157–170.

Sharif, M., Roberts, G., Sutton, R., 1994. Robust fin/rudder roll stabilization. Proc. IEEE 3rd Conference on Control Applications 2 (.), 1107—1112.

Sharif, M., Roberts, G., Sutton, R., 1995. Sea-trial experimental results of fin/rudder roll stabilization. Control Eng. Practice 3 (5), 703—708.

Sharif, M., Roberts, G., Sutton, R., 1996. Final experimental results of full scale fin/rudder rudder roll stabilisation sea trials. Control Engineerign Practice 4 (3), 377–384.

St Denis, M., Pierson, W., 1953. On the motion of ships in confused seas. SNAME Trans. 61, 280–332.

Stoustrup, J., Niemann, H., Blanke, M., 1995. A multi objective $\mathcal{H}_\infty$ solution to the rudder roll damping problem. In: Proc. of CAMS'95.

Taggart, R., 1970. Anomalous behavior of merchant ship steering systems. Marine Technology April, 205–215.

Tanguy, H., Lebret, G., Doucy, O., 2003. Multi-objective optimisation of pid and h_∞ fin/rudder roll controllers. In: 5th IFAC Conference on Manoeuvring and Control of Marine Craft MCMC'03.

van Amerongen, J., van der Klugt, P., van Nauta Lemke, H., 1990. Rudder roll stabilization for ships. Automatica 26, 679–690.

van der Klught, P., 1987. Rudder roll stabilization. Ph.D. thesis, Delft University of Technology, The Netherlands.

van der Klugt, P., 1987. Rudder roll stabilization. Ph.D. thesis, Delft University of Technology, The Netherlands.

van Gunsteren, F., 1974. Analysis of roll stabilizer performance. Trans. of The Society of Naval Architects and Marine Engineers 21, 125–146.

Vasta, J., Giddings, A., Taplin, A., Stilwell, J., 1961. Roll stabilization by means of passive tanks. Transactions of The Society of Naval Architects and Marine Engineers SNAME 69, 411–439.

Watt, P., 1883. On a method of reducing the rolling of ships at sea. Trans. of the Institution of Naval Architects 24.

Watt, P., 1885. The use of water chambers for reducing the rolling of ships at sea. Trans. of the Institution of Naval Architects 26.

Yang, C., Blanke, M., 1998. Rudder roll damping controller design using μ synthesis. In Proceeding of IFAC CAMS'98, 127–132.

Zhou, W., Chercas, D., Calisal, S., Tiano, A., 1990. A new approach for adaptive rudder roll stabilisation control. Proc. of the 9th Ship Control System Symposium 1, 115–127.